Three new palaeoniscoid fishes from the Bear Gulch Limestone (Serpukhovian, Mississippian) of Montana (USA) and the relationships of lower actinopterygians

Kathryn E. MICKLE
University of Kansas, Department of Ecology and Evolutionary Biology,
Natural History Museum and Biodiversity Research Center,
1345 Jayhawk boulevard, Lawrence, Kansas 66045 (USA)
kmickle@ku.edu

Richard LUND
18 Hillside road, Mount Holly, New Jersey 08060 (USA)
rlund@sju.edu

Eileen D. GROGAN
Saint Joseph's University, Department of Biology,
5600 City Line avenue, Philadelphia, Pennsylvania 19131 (USA)
egrogan@sju.edu

Mickle K. E., Lund R. & Grogan E. D. 2009. — Three new palaeoniscoid fishes from the Bear Gulch Limestone (Serpukhovian, Mississippian) of Montana (USA) and the relationships of lower actinopterygians. *Geodiversitas* 31 (3): 623-668.

ABSTRACT
Three new palaeoniscoid fishes (Osteichthyes, Actinopterygii), representing two new genera, *Lineagruan judithi* n. gen., n. sp., *L. snowyi* n. gen., n. sp., *Beagiascus pulcherrimus* n. gen., n. sp., are described from the Bear Gulch Limestone Member of the Heath Formation (Serpukhovian) of Montana, a 318 million year old lagerstätte. Morphological, morphometric, and meristic data were analyzed and compared to data for other Paleozoic actinopterygians. Differences among the species were noted in character complexes that may have played a role in feeding or propulsive regimes and fine-scale niche partitioning. A matrix of 111 characters and 40 taxa was constructed using relatively complete taxa ranging from the Devonian to the Recent. Cladistic analysis using Hennig86 and Winclada resulted in two trees. Branch-and-bound treatment generated one tree, in which the palaeoniscoids were paraphyletic. In all instances, the relationships of the three new species were consistent. It is noted that a number of the palaeoniscoid clades proposed by the current cladistic analysis have also been generated in earlier analyses of Bear Gulch fishes and other independent analyses. This recurring pattern implies some robustness to these associations in spite of variations between the matrices generating them.

KEY WORDS
Bear Gulch Limestone,
Palaeoniscoids,
lower actinopterygians,
Carboniferous,
Mississippian,
USA,
phylogeny,
new species,
new genera.

RÉSUMÉ
Trois nouveaux poissons palaeoniscoïdes du calcaire de Bear Gulch (Serpukhovian, Mississippien) du Montana et rapports entre actinoptérygiens inférieurs.
Trois nouveaux poissons palaeoniscoïdes (Osteichthyes, Actinopterygii), représentant deux nouveaux genres, *Lineagruan judithi* n. gen., n. sp., *L. snowyi* n. gen., n. sp., *Beagiascus pulcherrimus* n. gen., n. sp., sont décrits provenant du Calcaire de la Bear Gulch Formation de Heath (Serpukhovien) du Montana, gisement vieux de 318 millions d'années. Les données morphologiques, morphométriques, et méristiques sont analysées et comparées aux données d'autres actinoptérygiens paléozoïques. Les differences entre les espèces sont exprimées en complexes de caractères qui peuvent avoir joué un rôle dans les modes de nutrition et de propulsion, et dans la répartition en des niches de petite taille. Une matrice de 111 caractères et 40 taxons est élaborée en utilisant des taxons relativement complets allant du Dévonien à l'époque actuelle. Une analyse cladistique utilisant Hennig 86 et Winclada aboutit à deux arbres. Le traitement "branch-and-bound" a généré un arbre, dans lequel les paléoniscoïdes sont paraphylétiques. Dans tous les cas, les relations des trois nouvelles espèces sont cohérentes. Il est à noter qu'un certain nombre de clades de paléoniscoïdes résultant de la présente analyse cladistique ont également été générés par des analyses antérieures des poissons de Bear Gulch et par d'autres analyses indépendantes. Ce modèle récurrent accorde quelque robustesse à ces associations en dépit des différences des matrices qui les ont générées.

MOTS CLÉS
Calcaire de Bear Gulch,
paléoniscoïdes,
Actinoptérygiens
inférieurs,
Carbonifère,
Mississippien,
USA,
phylogénie,
espèces nouvelles,
genres nouveaux.

INTRODUCTION

The term palaeoniscoid refers to a group of more than 250 extinct genera of lower actinopterygian fishes ranging from the Late Silurian to the Cretaceous that share a similar body shape and arrangement of cranial bones (Janvier 2002; Poplin & Lund 2002). They are typically characterized by the presence of an immovable maxilla-preoperculum-hyomandibula-palate structure, a fusiform or elongate fusiform or deep body shape, a single triangular or elongated dorsal and anal fin, a heterocercal caudal fin, and articulated rhombic scales (Schaeffer & Rosen 1961; Moy-Thomas & Miles 1971; Janvier 2002).

Moy-Thomas & Miles (1971) recognized the palaeoniscoids as representative of the ancestral actinopterygian condition. Gardiner (1984) and Zhu & Schultze (2001) later proposed that the palaeoniscoids may provide a greater understanding of both the early actinopterygian condition and the original osteichthyan plan. Yet, most studies of the interrelationships of Paleozoic lower actinopterygians have been hindered by few and/or poorly preserved specimens. In contrast, the Bear Gulch Limestone of Montana (Serpukhovian, Namurian E2b) preserves a diverse assemblage of well-preserved actinopterygians.

The Lower Carboniferous Bear Gulch Limestone beds (*c.* 318 million years old) are one of a number of limestone lenses that make up the Bear Gulch Limestone Member of the Heath Formation of Montana and North Dakota (Grogan & Lund 2002). The Heath Formation and underlying Otter and Kibbee Formations are Serpukhovian (Namurian E2b) in age (Lund & Poplin 1997; Grogan & Lund 2002; Poplin & Lund 2002). The Bear Gulch Limestone was deposited in a shallow Paleozoic tropical marine bay located 12°N of the equator that contained a diverse marine flora and fauna (Williams 1983; Lund & Poplin 1999; Grogan & Lund 2002). Field excavations over 39 years have revealed an ichthyofauna with over 5500 specimens of fishes from over 125 species (Lund 2000; Grogan & Lund 2002). Actinopterygians constitute approximately 72% of recovered specimens but

only 33% of putative species. The abundance and diversity of actinopterygian material alone sets the Bear Gulch apart from other Paleozoic deposits around the world (Lund & Poplin 1997).

Three previously undescribed Bear Gulch palaeoniscoids are now described. Extensive morphometric parameters are explored for their potential utility in identification and objective description. The phylogenetic relationship of these fishes to other actinopterygians is also investigated.

Bone nomenclature

Traditional and topographic actinopterygian bone nomenclature is used to limit contention over inferred bone homologies. Frontal and parietal are used rather than parietal and postparietal, respectively. The terms posteroventral infraorbital and posterodorsal infraorbital are used to refer to the bones bearing the infraorbital canal that are located in the posteroventral and posterodorsal corners of the orbit, respectively, following the scheme presented by Poplin & Lund (2002). Posterodorsal infraorbital is used instead of dermosphenotic, because the former name pertains to a cheek bone rather than a skull roofing bone, as in these fishes. The two bones in the skull roof that carry the otic canal are referred to as the dermosphenotic and dermopterotic rather than the intertemporal and supratemporal, respectively. (For another view on the dermosphenotic and dermopterotic, see Poplin [2004]). The terms basal fulcra, fringing fulcra, and procurrent fin rays are used following the scheme presented by Schultze & Arratia (1989) and Arratia (2008).

Abbreviations

CM	Carnegie Museum of Natural History, Pittsburgh;
MV	University of Montana Geological Museum, Missoula;
ROM	Royal Ontario Museum, Toronto.

MATERIALS AND METHODS

Fossils were examined by stereomicroscopy and occasionally viewed under 70% ethanol to aid in the visualization of select features. Digitized images were prepared by scanning the fossils with a Microtek 4800 × 3200 PPI flatbed scanner or using a Canon XSi digital camera with a macro lens. Meristic counts and morphometric measurements were taken directly from original specimens according to Poplin & Lund (2002). A series of potentially braincase-independent lateral cranial measurements were added to this measurement scheme to maximize the recovery of objective data for analyses (Fig. 1). Cranial measurements were performed upon high-resolution scans of specimen heads, using the measure function of Adobe Illustrator software. Where possible, latex peels were prepared to provide three dimensional views of specimens preserved from negative impressions. These were shadowed with magnesium oxide and examined in parallel with original specimens. Original specimens and latex peels were used to prepare drawings and illustrations using Adobe Photoshop and Adobe Illustrator softwares.

Statistical analyses of measurements and graphs of morphometric and meristic data were prepared using SPSS software. The classification function of Discriminant Analysis was used to determine whether the variables supported the three proposed species. Principle Component Analysis identified what factors (combinations of variables) best defined the three species (Harris 1975).

A cladistic matrix (111 characters, 40 taxa; Appendix 1) was constructed to examine the interrelationships of lower actinopterygian fishes. This matrix of 83 cranial and 28 postcranial characters includes Bear Gulch and non-Bear Gulch actinopterygians. Trees were rooted on four outgroups – a hypothetical outgroup and three sarcopterygians. The ingroup included 36 taxa of extinct and extant actinopterygians that range from the Devonian to Recent (Appendix 4).

Cladistic analysis was performed using Hennig86 (Farris 1986) and Winclada (Nixon 2002). In Hennig86, all characters were run non-additively with the mh* procedure. Branch-and-bound treatment was also performed on the resulting trees. Trees were viewed and analyzed with Winclada (Nixon 2002).

SYSTEMATICS

Class OSTEICHTHYES Huxley, 1880
Subclass ACTINOPTERYGII Cope, 1891
Family *incertae sedis*

Genus *Lineagruan* n. gen.

TYPE SPECIES. — *Lineagruan judithi* n. sp.

OTHER INCLUDED SPECIES. — *Lineagruan snowyi* n. sp.

ETYMOLOGY. — *Lineagruan*, meaning lined cheek, referring to the fine, vertical ganoine pattern on the cheek region. From *linea*, *lineach*, Latin, Gaelic for lined, and *grua*, Gaelic for cheek.

DIAGNOSIS. — A lower actinopterygian fish defined by the following combination of characters: elongate fusiform body; paired toothed premaxillae sutured in midline; single median rostropostrostral; rhombic antorbital; dermopterotic with anterior process situated within notch in frontal; three infraorbitals, T-shaped posterodorsal infraorbital with single spiracular bone situated between posterior arms; three suborbitals – two large suborbitals in curve of preoperculum, one small intervening suborbital between maxilla and posteroventral infraorbital; tall, rounded posterior plate of maxilla with pronounced posteroventral process; operculum taller than subopercular; dorsal margin of subopercular sinusoidal; operculum and subopercular bear continuous fine vertical ganoine ridges; postspiracular sutured to dorsal portion of operculum; extralateral gular present; median fins originating more than halfway down body length; dorsal fin originates anterior to anal fin; paired and unpaired fins bear short, thin fringing fulcra on leading edges; guard scales on dorsal and anal fin bases; caudal fin heterocercal, deeply cleft, and nearly equilobate with fringing fulcra on dorsal and ventral lobes and large accessory flap on epicaudal lobe.

REMARKS

Some specimens included in this genus were originally designated in an unpublished Ph.D. thesis as a single species, "*Mesopoma becketense*" (Lowney 1980). Neither Lowney's original reconstruction nor this material justifies its assignment to the genus *Mesopoma* (Coates 1993).

Lineagruan judithi n. sp.
(Figs 2-5; 6A; Tables 1-4)

HOLOTYPE. — CM 35412.

ETYMOLOGY. — *Lineagruan judithi* n. sp., named for the Judith Mountains of Montana.

REFERRED SPECIMENS. — CM 27401, CM 35408, CM 35595, CM 35596, CM 37592, CM 40997, CM 40998, CM 46034, CM 46035, CM 46104, CM 46115, CM 48546, CM 48765, CM 48768, CM 48793, CM 62743, CM 62880, CM 63048, CM 63049, CM 63078, CM 78509; MV 3630, MV 6132, MV 6133, MV 6372, MV 6927, MV 6936, MV 7657; ROM 41823, ROM 43128.

OCCURRENCE. — Upper Mississippian (Serpukhovian, Namurian E2b) Bear Gulch Limestone lens, Bear Gulch Limestone Member of the Heath Formation, Big Snowy Group, southwest of Becket, Fergus County, Montana (USA).

DIAGNOSIS. — Meristic, morphometric, and cranial measurements are presented in Tables 1 to 4. Total length ranges from 4.1-9.5 cm; deep sulcus on skull roof at the median suture between frontals; small, triangular dermosphenotic; large dermopterotic with short, thin anterior arm extending anterodorsally into frontal; relatively vertical posterior margin of maxilla; preopercular angle 45°; opercular angle 54°; subopercular angle 82.9°; between and within specimens, the operculum and suboperculum may or may not be fused; vertically oriented hyomandibula; thin block shaped anteopercular bones along anterior margin of operculum – first anteopercular expanded; 4-6 branchiostegal rays below mandible; extrascapulars vary in numbers of rows and numbers of bones between and within specimens; flank scales with on average six pronounced serrations; maxilla and preoperculum with roughly vertical ganoine ridges; ridge scales anterior to dorsal and caudal fins; slight accessory lobe on epicaudal lobe of caudal fin.

DESCRIPTION

Body form (Figs 2; 3)

The body is elongate-fusiform in shape. Specimens are preserved in lateral, dorsal, and ventral views that show these fish were round in cross section. Median fins are set far back on the body, with the dorsal fin originating anterior to the anal fin. Meritic and morphometric data are found in Tables 1 and 2.

Snout (Figs 2; 4)

Small, wedge-shaped, toothed premaxillae lie ventral to the rostropostrostral and are sutured in midline-forming the anterior-most margin of the mouth. The antorbital has a narrow vertical process that extends up to the posteroventral border of the nasal

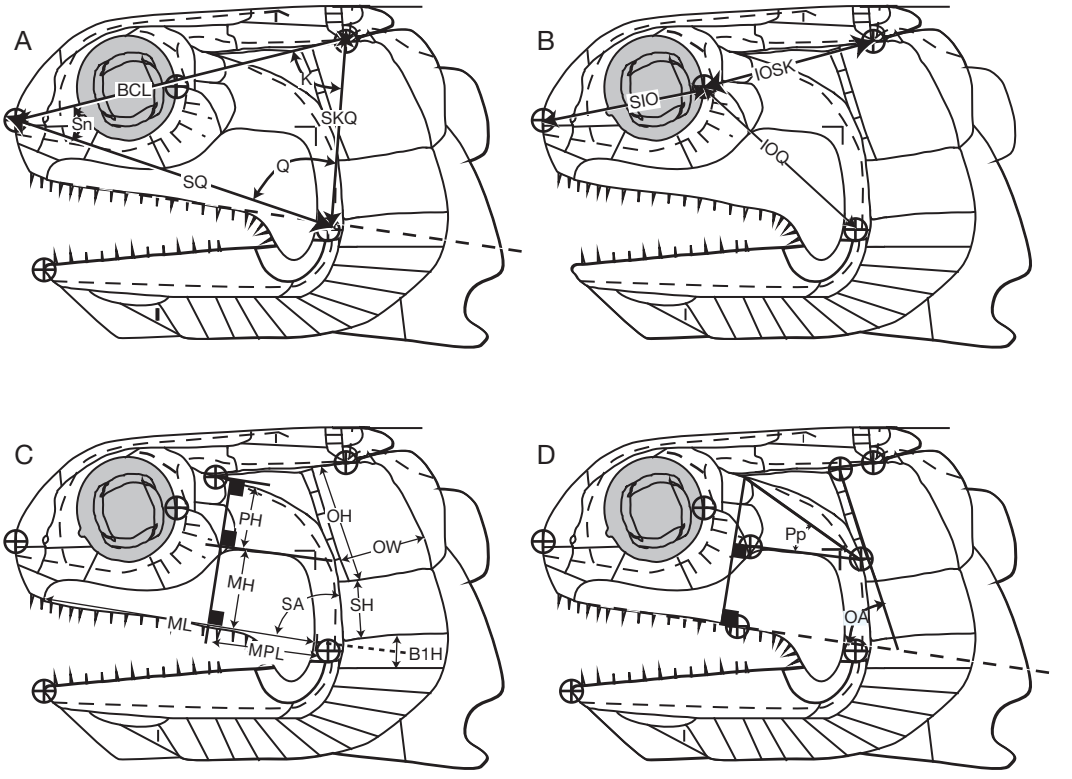

Fig. 1. — Cranial measurements, figure modified from Lund & Poplin (1997): **A**, external cranial triangle; **B**, internal cranial triangles; **C**, cheek measures; **D**, maxillary, preopercular and opercular measures. Abbreviations: **B1H**, height of first branchiostegal; **BCL**, braincase length; **IOQ**, infraorbital to quadrate length; **IOSK**, length from the dorsal border of the posteroventral infraorbital to the posterolateral corner of skull; **K**, angle of skull roof; **MH**, height of maxilla; **ML**, maxilla length; **MPL**, length of maxillary process; **OA**, angle of operculum; **OH**, height of operculum; **OW**, width of operculum; **PH**, height of preoperculum; **Pp**, angle of preoperculum; **Q**, quadrate; **SA**, subopercular angle; **SH**, suboperculum height; **SIO**, snout to infraorbital length; **SKQ**, length from posterolateral corner of skull roof to quadrate; **Sn**, snout; **SQ**, snout to quadrate length. Circles represent landmarks used to make measurements.

and a horizontal portion that extends anteriorly up to the rostropostrostral. The nasal is situated within the curve created by the vertical and horizontal portions of the antorbital. The antorbital bears a Y-shaped tripartite canal formed by the junction of the infraorbital and supraorbital canals and the ethmoid commissure.

The nasal lies dorsal to the antorbital and lateral to the rostropostrostral and carries the supraorbital canal along its anterior margin from the antorbital to the frontal. The posterior tip of the nasal is anterior to, but does not come in contact with, the tip of the posterodorsal infraorbital as a result of a small spur on the frontal. Ventrally, the nasal is notched for the anterior and posterior nasal openings. A single median rostropostrostral bearing the ethmoid commissure is ventral to the frontal and dorsal to the paired premaxillae. The rostropostrostral extends dorsally to mid-orbit and is notched ventrolaterally for the anterior nasal openings.

Three heavily ossified sclerotic bones are present. A fourth sclerotic on the anterior-most margin of the orbit is not seen – whether a fourth sclerotic was present but unossified is unclear.

Skull roof (Figs 2; 4)

The ventrally flared lateral margins of the skull roof make the skull roof appear dome-like. There

TABLE 1. — *Lineagruan judithi* n. gen., n. sp., meristic counts. Abbreviations: **AFP**, anal fin position; **CFP**, caudal fin position (number of scales in lateral line to the caudal fin); **DFP**, dorsal fin position; **N**, number of specimens; **NAN**, number of anal fin rays; **NCAU**, number of caudal fin rays; **NDOR**, number of dorsal fin rays; **NP1**, number of pectoral fin rays; **NP2**, number of pelvic fin rays; **P2P**, pelvic fin position; **SAL**, scales to dorsal origin above lateral line; **SBL**, scales to anal origin below lateral line; **ST DEV**, standard deviation. Counts taken from Poplin & Lund (2002).

	DFP	AFP	CFP	P2P	NP1	NP2	SBL	SAL	NDOR	NAN	NCAU
Mean	23	20	45	11	18	12	15	12	28	28	56
Min	21	18	41	10	16	9	10	8	22	21	42
Max	25	23	50	13	20	16	17	17	35	35	66
N	15	13	10	5	4	3	14	13	4	12	6
ST DEV	1.34	1.27	2.69	1.23	1.63	3.61	1.92	3.11	5.38	4.47	10.03

TABLE 2. — *Lineagruan judithi* n. gen., n. sp., natural logarithms of morphometric measurements (in cm). Abbreviations: **ABAS**, length of anal fin base; **AOCV**, anal fin origin to origin of the ventral lobe of the caudal fin; **CBAS**, length of caudal fin base; **CPL**, caudal peduncle length; **CPW**, caudal peduncle width; **DBAS**, length of dorsal fin base; **DOCD**, distance from the origin of the dorsal fin to origin of the caudal fin; **FORK**, distance from snout to fork of caudal fin; **HTDO**, height of the body at the origin of the dorsal fin; **MXHT**, maximum height; **P1P2**, distance from the origin of the pectoral fin to the origin of the pelvic fin; **P2AO**, distance from the origin of the pelvic fin to the origin of anal fin; **SAO**, distance from the snout to the origin of the anal fin; **SDO**, distance from the snout to the origin of dorsal fin; **SL** standard length; **SP1**, distance from the snout to the origin of the pectoral fin; **SP2**, distance from the snout to origin of the pelvic fin. Measurements taken from Poplin & Lund (2002).

	ABAS	AOCV	CBAS	CPL	CPW	DBAS	DOCD	FORK	HTDO	MXHT	P1P2	P2AO	SAO	SDO	SL	SP1	SP2
Mean	0.09	0.74	0.87	-0.05	-0.17	0.09	1.07	2.17	0.67	0.92	0.82	0.69	1.72	1.52	2.09	0.7	1.47
Min	-0.51	0.10	0.10	-0.69	-0.69	-0.36	0.41	1.50	0.18	0.26	0.74	0.34	1.10	0.92	1.41	0.10	1.41
Max	0.53	0.99	1.16	0.47	0	0.53	1.36	2.31	0.92	1.25	1.03	1.03	1.9	1.7	2.25	0.96	1.53
N	18	11	14	10	13	11	12	14	8	11	7	8	17	15	17	20	8
ST DEV	0.32	0.24	0.25	0.33	0.18	0.28	0.24	0.20	0.22	0.25	0.12	0.21	0.19	0.19	0.19	0.18	0.04

TABLE 3. — Cranial measurements (in mm) for *Lineagruan judithi* n. gen., n. sp., natural logarithms of cranial triangle and individual bone measurements. Abbreviations: **B1H**, height of first branchiostegal; **BCL**, brain case length; **IOQ**, infraorbital to quadrate length; **IOSK**, length from the dorsal border of the posteroventral infraorbital to the posterolateral corner of skull; **MH**, height of maxilla; **ML**, maxilla length; **MPL**, length of maxillary process; **OH**, height of operculum; **OW**, width of operculum; **PH**, height of preoperculum; **SH**, height of suboperculum; **SIO**, length from the snout to the infraorbital length; **SKQ**, length from the posterolateral corner of the skull roof to snout length; **SQ**, length from the snout to quadrate length.

	BCL	B1H	IOQ	MH	ML	MPL	OH	OW	PH	SH	SIO	IOSK	SKQ	SQ
Mean	2.72	0.10	2.19	1.31	2.65	1.70	2.07	1.62	1.16	1.04	2.19	2.01	2.46	2.79
Min	2.53	-0.41	1.73	1.07	2.48	1.22	1.92	1.47	0.61	0.78	2.04	1.81	2.27	2.45
Max	3.06	0.60	2.54	1.75	3.19	2.54	2.44	1.83	1.50	1.27	2.67	2.28	2.75	3.27
N	11	2	10	12	13	11	12	13	10	7	10	10	11	11
ST DEV	0.13	0.72	0.21	0.21	0.18	0.33	0.15	0.11	0.29	0.17	0.17	0.13	0.15	0.20

TABLE 4. — Cranial measurements for *Lineagruan judithi* n. gen., n. sp., cranial angles. Abbreviations: **K**, angle of the skull roof; **OA**, angle of operculum; **Pp**, angle of preoperculum; **Q**, quadrate; **SA**, subopercular angle; **Sn**, snout.

	K	OA	Pp	Q	Sn	SA
Mean	76.36	53.34	43.78	62.75	41.25	78.54
Min	61.45	40.73	33.32	53.07	34.74	49.72
Max	91.75	71.09	53.00	71.38	47.27	93.87
N	11	10	8	11	10	7
ST DEV	9.57	9.81	6.25	6.64	4.06	15.35

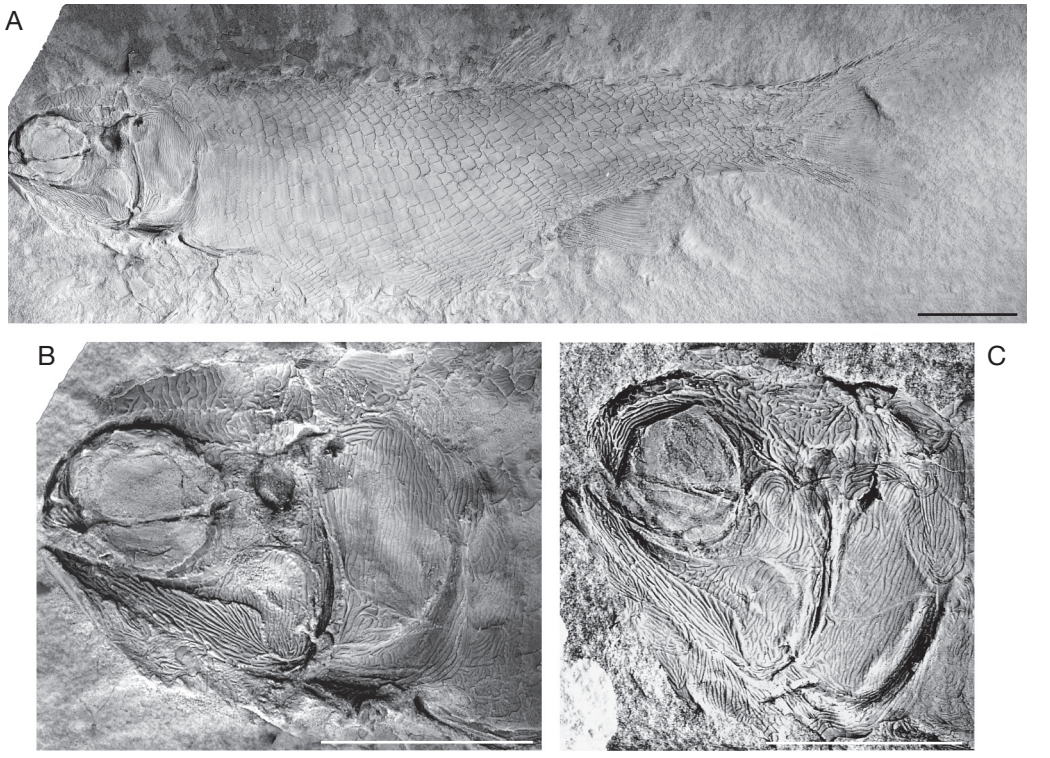

FIG. 2. — *Lineagruan judithi* n. gen., n. sp.: **A**, **B**, holotype (CM 35412); **A**, left view of the whole fish, natural cast; **B**, natural cast of the left lateral view of the head; **C**, CM 62743A, natural cast of the left lateral view of the head. Scale bars: 1 cm.

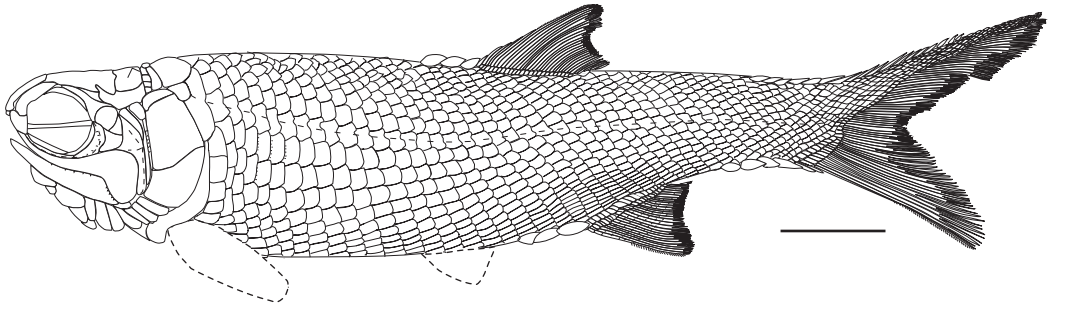

FIG. 3. — *Lineagruan judithi* n. gen., n. sp., reconstruction based upon holotype (CM 35412) and CM 62743. Scale bar: 1 cm.

is also a deep median sulcus. The frontal is paired with an intervening sinusoidal sagittal suture. In lateral view, the frontal is wider posteriorly than anteriorly. The posterior margin of the frontal is notched to accommodate the anteromedial aspect of the parietal bone; the supraorbital canal can be seen exiting the frontal and entering the parietal at this notch. The lateral margin of the frontal is curved and notched for the reception of the anterodorsal process of the dermopterotic. Anterior

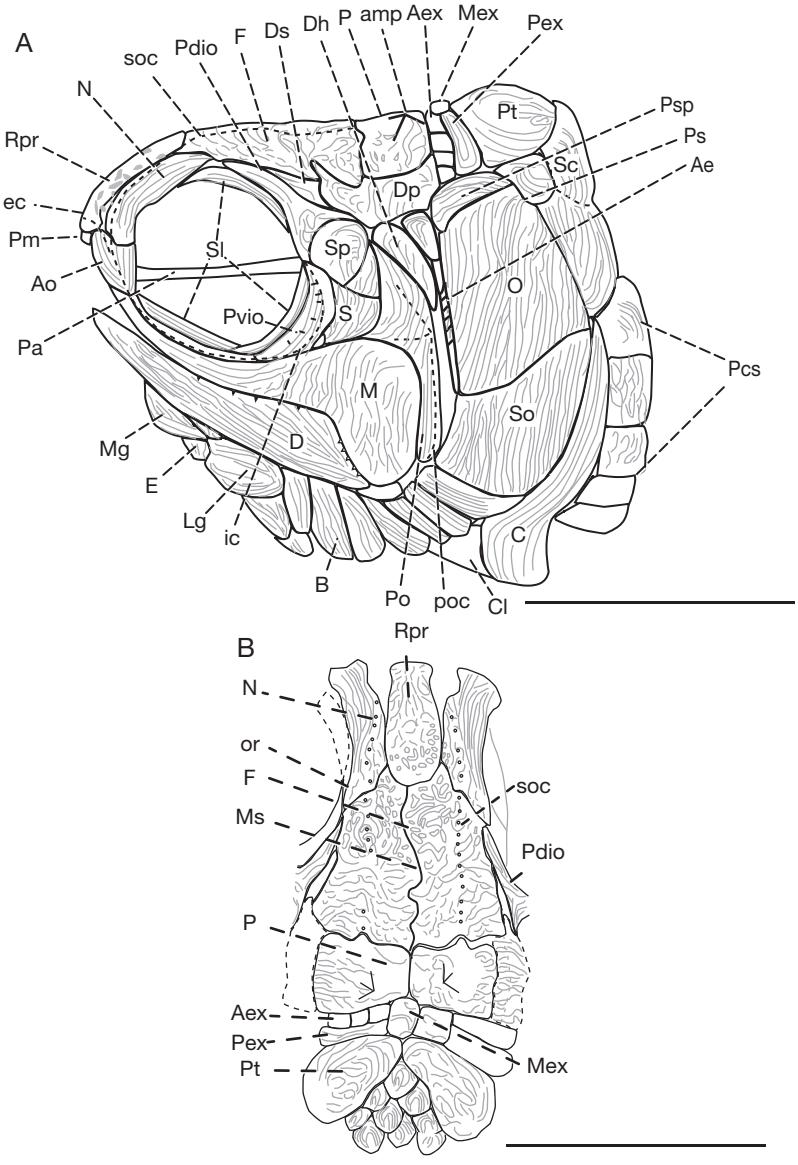

FIG. 4. — *Lineagruan judithi* n. sp.: **A**, reconstruction of the head in lateral view based upon CM 62743 A and holotype (CM 35412 A); **B**, dorsal surface of the head of MV 6133. Note bilateral asymmetry of anterior extrascapulars. Bone names in capital letters, canal lines in lower case letters. Abbreviations: **Ae**, anteopercular bones; **Aex**, anterior extrascapulars; **amp**, anterior, median, posterior parietal pit lines; **Ao**, antorbital; **B**, branchiostegal rays, **C**, cleithrum; **Cl**, clavicle; **D**, dentary; **Dh**, dermohyal; **Dp**, dermopterotic; **Ds**, dermosphenotic; **E**, extralateral gular; **ec**, ethmoid commissure; **F**, frontal; **ic**, infraorbital canal; **Lg**, lateral gular; **M**, maxilla; **Mex**, median extrascapular; **Mg**, median gular; **Ms**, median sulcus; **N**, nasal; **O**, operculum; **or**, orbit; **P**, parietal; **Pa**, parasphenoid; **Pcs**, postcleithral scales; **Pdio**, posterodorsal infraorbital; **Pex**, posterior extrascapulars; **Po**, preoperculum; **poc**, preopercular canal; **Pm**, premaxilla; **Ps**, presupracleithrum; **Psp**, postspiracular; **Pt**, posttemporal; **Pvio**, posteroventral infraorbital; **Rpr**, rostropostrostral; **S**, suborbital; **Sl**, sclerotic; **So**, suboperculum; **soc**, supraorbital canal; **Sp**, spiracular covering. Scale bars: 1 cm.

to the dermopterotic process, the frontal widens, only to be notched again by the anterior tip of the dermosphenotic. The parietal is rhombic with rounded corners, has a small anterior bulge situated within a notch in the frontal, and a small spur on the lateral margin. The suture between the parietal and dermopterotic is sinusoidal. The parietal bears the characteristic tripartite pit line formed by the anterior, middle, and posterior pit lines. The dermosphenotic is a thin, tapered, triangular bone dorsal to the posterodorsal infraorbital. The posteroventral infraorbital does not contact the nasal because of an intervening small spur of the frontal. The dermosphenotic is curved where it contacts the dermopterotic posteriorly.

The dermopterotic is a large bone ventrolateral to the frontal and parietal with a thin process that extends anterodorsally into a notch in the lateral margin of the frontal bone. It is taller posterior to the flared portion of the frontal.

Cheek (Figs 2; 4)

There are three infraorbitals that bear the infraorbital canal – a thin, narrow bone ventral to the orbit, a posteroventral, and a posterodorsal infraorbital. The posteroventral infraorbital is a crescent-shaped bone with clear radiating pore lines. The posterodorsal infraorbital is T-shaped and tapers to a point anteriorly. A large round spiracular bone is situated within the curved arms of the posterodorsal infraorbital and dorsal to the suborbitals. Two triangular suborbitals are situated within the anterior curved arms of the preoperculum. A third, smaller, intervening suborbital is inserted between the posteroventral infraorbital and maxilla.

The preoperculum is hatchet-shaped due to a narrow vertical section that curves anteriorly at its dorsal-most and ventral-most extent. The dorsal curvature occurs over a greater span than the ventral – the average angle between the two limbs is 45°. The narrow vertical section of the preoperculum carries the preopercular canal into the expanded dorsal region. The short, horizontal pit line is seen on the expanded region of the preoperculum. The maxilla is long with a tall rounded posterior plate and a pronounced posteroventral process. Anteriorly, the maxilla tapers to a curved narrow arm ventral to the orbit. Two rows of acrodont, conical, vertically oriented teeth line the oral margin of the maxilla-small lateral and larger medial teeth. Near the maxillary fossa, the ventral process of the maxilla is lined with anteriorly oriented, short, pointed teeth.

The dentary is wider posteriorly and gradually tapers to a rounded point anteriorly. Minute teeth are along the dentary in at least one specimen, CM 27401. In one specimen, CM 35412, the maxilla has been displaced, allowing for visualization of the posterior end of the mandible and the articular. The quadrate is situated dorsal to the articular. The symplectic is seen dorsal to the quadrate and ventral to the preoperculum and presumptive ventral end of the hyomandibula.

A wedge-shaped dermohyal is seen posterior to the preoperculum and anterior to the hyomandibula. The dermohyal is rounded dorsally, tapers to a point ventrally, and extends ventrally to about the mid point of the operculum. Though thin, a row of anteopercular bones are found along the anterior margin of the operculum. Delicate, distinct ganoine patterns can be seen on each block. The first anteopercular bone is an exception – it is expanded and bears clear ganoine ridges. While a majority of the specimens have anteopercular bones along the height of the operculum, anteopercular bones of CM 63078 extend the height of both operculum and suboperculum.

Operculo-gular apparatus (Figs 2; 4; 5; 6A)

The operculum is a rectangular bone that is wider ventrally than dorsally and situated at an angle of 54°. Due to the sigmoidal suture with the suboperculum, the operculum is taller anteriorly than posteriorly. The suboperculum has a convex lower suture and is situated at an angle of 82.9°. The operculum and suboperculum are subject to intraspecific variation, ranging from unfused to fused conditions (Fig. 5) and such variation may be found between right and left sides of the same specimen. The fused condition is caused by a continuous layer of ganoine covering the operculum and suboperculum. The internal view of the bones shows that they are separated while the external view shows a continuous thick layer of ganoine that covered both of the bones making them function as one unit. A crescent-shaped postspiracular bone with a distinctive ganoine pattern is sutured dorsally to the operculum.

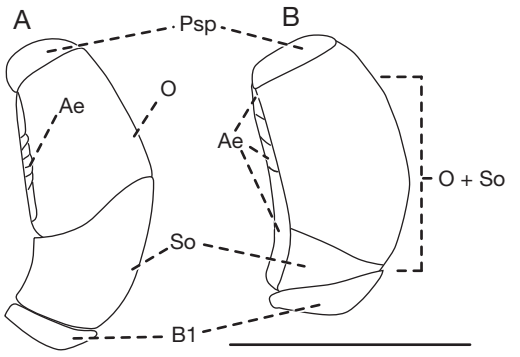

FIG. 5. — Opercular/subopercular conditions in *Lineagruan judith* n. gen., n. sp.: **A**, operculum and suboperculum unfused, illustration based on CM 62743; **B**, operculum and suboperculum fused, illustration based on CM 35412 A. Abbreviation: **B1**, first branchiostegal ray. See Figure 4 for abbreviations. Scale bar: 1 cm.

A series of 4-6 branchiostegal rays extends ventrally from the suboperculum to the posterior ⅓ of the ventral margin of the dentary. The first branchiostegal ray is slightly wider than the other rays. An oval-shaped median gular is present, as well as two contralateral pairs of oval-shaped lateral gulars and a pair of extralateral gulars. The gulars extend approximately ⅔ down the ventral margin of the dentary (Fig. 6A).

Pectoral girdle (Fig. 4)

The extrascapulars are characterized by intraspecific variation as well as bilateral asymmetry. The most prevalent condition is to have an anterior extrascapular row and a posterior row sharing a single median extrascapular. The anterior extrascapular row is composed of 2-3 anamestic block-like bones. The posterior extrascapular row is a single rectangular band of bones that bears the supratemporal commissure, which often displays radiating pore canal lines. CM 48768 bears a single row of four lateral extrascapulars separated by a median extrascapular. The right side of the head of CM 37592 has three bones in the anterior extrascapular row while the left side has two bones in the same row.

The posttemporals are paired bones posterior to the extrascapulars. When viewed laterally, the posttemporal appears as a rounded, acuminate bone. When viewed dorsally, the posttemporals are seen as rounded triangular bones that are wider laterally than medially. A rounded presupracleithrum is present posterodorsal to the operculum, anterior to the supracleithrum, and ventral to the posttemporal. The anteroventral margin of the bone is covered by the operculum. The supracleithrum is an elliptical bone that is notched at the exit point of the trunk lateral line. The supracleithrum is about the same height as the operculum, but the anterior half of the supracleithrum is covered by the operculum. The cleithrum extends from the ventral margin of the supracleithrum to the posterior margin of the clavicle and bears a ventral notch to accommodate the pectoral fin. It is often covered by the suboperculum and branchiostegal rays. A wide clavicle is apparent as a triangular bone anterior to the cleithrum and mesial to the branchiostegal rays.

Suspensorium

In CM 35412 and CM 62743, the hyomandibula extends from the skull roof just ventral to the dermopterotic, to the inferior tip of the preoperculum. The hyomandibula is roughly vertical in orientation, following the posterior margin of the preoperculum.

Squamation (Fig. 4)

A row of rhombic postcleithral scales with circumferential ganoine ridges are present ventral to the supracleithrum and continue ventrally down the length of the cleithrum. Anteriorly placed flank scales are rectangular, finely pectinated on the posterior edge, with an average of six serrations per scale, and bear longitudinal ridges. Ventral scales are narrow and rectangular. An abrupt inversion in the direction of the scale rows occurs in the caudal peduncle at scale row 43.

Fins

The pectoral and pelvic fins both bear short, fine fringing fulcra on their leading edges. The pelvic fin is small and roughly rectangular. Median fins are triangular and are set more than halfway down the standard length of the body (Tables 1; 2). The dorsal fin originates anterior to the anal fin. Both dorsal and anal fin bases are composed of rectangular guard scales. Short unjointed basal fulcra form the leading edges of the fins. Posterior to the basal fulcra, the leading edges of both the dorsal and anal

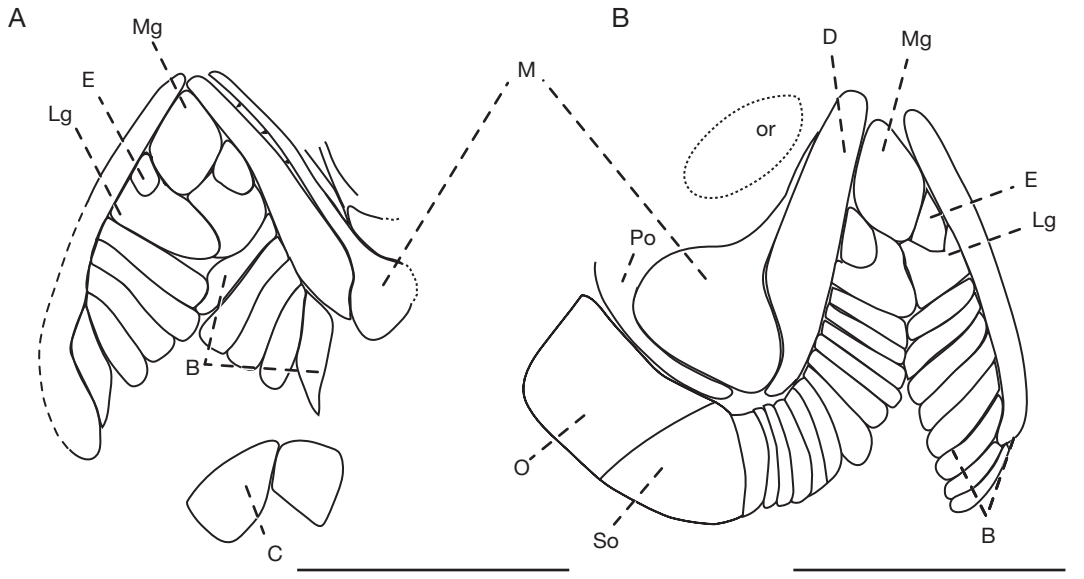

FIG. 6. — **A**, *Lineagruan judithi* n. gen., n. sp., illustration based upon CM 40998; **B**, *Lineagruan snowyi* n. gen., n. sp., illustration based upon CM 35406; **A**, **B**, ventral views. See Figure 4 for abbreviations. Scale bars: 1 cm.

fin are lined with short fringing fulcra. The rays of both the dorsal and anal fins are thin, jointed, and divided distally. The anal and dorsal fins gradually taper posteriorly. At least four rounded ridge scales are present anterior to the dorsal fin.

The heterocercal, deeply cleft, and slightly inequilobate caudal fin is preceded by at least five rounded, overlapping dorsal ridge scales. Posterior to these, basal fulcra line the anterior half of the scaled lobe. The posterior half of the scaled lobe bears short, fine, fringing fulcra. Along the ventral margin of the body in front of the caudal fin, at least four ridge scales are seen. The ventral lobe of the caudal fin bears short, fine fringing fulcra down its entire margin. A slight accessory lobe, or an area of longer lepidotrichia at the tip of the dorsal lobe, can be seen on the epicaudal lobe of some specimens.

Neurocranium

Well ossified neurocrania are preserved in two specimens, CM 35412 and CM 63078, revealing the articulation with the hyomandibula. A deep concavity lies posterior to the orbit, lateral to the ascending wing of the parasphenoid, and ventral to the posterodorsal infraorbital (CM 35412). The ventral component of this pit appears to be the posterior myodome. Dorsal to the myodome is another concavity that may have been associated with blood vessels or nerves. In this area and in the orbit, dark rust coloured pigments can be seen, suggesting preservation of blood-derived pigments (Grogan & Lund 2002). This entire postorbital area is typically covered by the large spiracular covering. The posterior dorsal edge of the braincase is excavated for a shallow posttemporal fossa that is roofed by the anterior extrascapulars.

An otolith is preserved in CM 62743 B as a yellow protuberance ventral to the dermosphenotic and dorsal to the preoperculum. Other specimens (CM 35412, MV 6372) have evidence of otoliths preserved as bulges or pits in the otic region.

Lineagruan snowyi n. sp.
(Figs 6B; 7-9; Tables 5-8)

HOLOTYPE. — ROM 41809.

ETYMOLOGY. — *Snowyi,* from the Big Snowy Mountains of Montana**.**

TABLE 5. — *Lineagruan snowyi* n. gen., n. sp., meristics counts. Abbreviations: see Table 1.

	DFP	AFP	CFP	P2P	NP1	NP2	SBL	SAL	NDOR	NAN	NCAU
Mean	26	20	48	12	28	11	20	15	34	30	62
Min	24	18	44	11	28	9	20	13	33	23	54
Max	27	25	49	12	28	13	20	17	36	37	64
N	4	5	4	2	1	3	2	2	3	3	5
ST DEV	1.29	2.7	2.38	0.71	–	2.08	0	2.83	1.73	7.02	5.63

TABLE 6. — *Lineagruan snowyi* n. gen., n. sp., natural logarithms of morphometric measurements (in cm). Abbreviations: see Table 2.

	ABAS	AOCV	CBAS	CPL	CPW	DBAS	DOCD	FORK	HTDO	MXHT	P1P2	P2AO	SAO	SDO	SL	SP1	SP2
Mean	0.42	1.12	1.27	0.44	0.09	0.77	1.45	2.48	0.97	0.99	0.83	0.74	2.01	1.82	2.38	1.06	1.61
Min	0.26	1.10	1.13	0.34	0	0.59	1.34	2.40	0.83	0.88	0.83	0.74	1.93	1.76	2.21	0.88	1.50
Max	0.59	1.16	1.44	0.53	0.18	0.88	1.61	2.57	1.19	1.16	0.83	0.74	2.12	1.89	2.51	1.13	1.67
N	5	5	3	5	5	3	4	4	5	5	2	2	5	5	6	6	3
ST DEV	0.13	0.03	0.15	0.07	0.09	0.16	0.13	0.08	0.15	0.13	0	0	0.08	0.06	0.10	0.09	0.09

TABLE 7. — Cranial measurements for *Lineagruan snowyi* n. gen., n. sp., natural logarithms of cranial triangle and individual bone measurements (in mm). Abbreviations: see Table 3.

	BCL	B1H	IOQ	MH	ML	MPL	OH	OW	PH	SH	SIO	IOSK	SKQ	SQ
Mean	2.92	0.53	2.51	1.50	2.99	2.12	2.27	1.76	1.30	1.27	2.47	2.09	2.64	3.13
Min	2.82	0.53	2.25	1.32	2.91	1.95	2.16	1.64	1.17	1.01	2.31	1.78	2.44	3.03
Max	3.04	0.53	2.69	1.79	3.13	2.37	2.36	1.87	1.48	1.36	2.53	2.27	2.78	3.21
N	4	1	4	5	5	5	5	4	5	4	4	4	4	4
ST DEV	0.09	0	0.20	0.20	0.09	0.17	0.09	0.10	0.12	0.17	0.11	0.23	0.16	0.07

TABLE 8. — Cranial measurements for *Lineagruan snowyi* n. gen., n. sp., cranial angles. Abbreviations: see Table 4.

	K	OA	Pp	Q	Sn	SA
Mean	86.76	44.64	38.95	54.62	38.77	64.25
Min	83.52	50.64	30.33	51.79	34.74	57.71
Max	91.75	37.52	48.00	57.19	44.47	71.80
N	4	4	4	4	4	4
ST DEV	3.78	5.40	7.46	2.6	4.58	6.32

REFERRED SPECIMENS. — CM 27377, CM 35406, CM 35449, CM 40999, CM 63050, MV 2969, MV 2980, MV 6119, MV 7010.

OCCURRENCE. — Upper Mississippian (Serpukhovian, Namurian E2b) Bear Gulch Limestone lens, Bear Gulch Limestone Member of the Heath Formation, Big Snowy Group, southwest of Becket, Fergus County, Montana (USA).

DIAGNOSIS. — Meristic, morphometric, and cranial measurements are presented in Tables 5 to 8. Body length ranges from 9.1 to 12.3 cm; antorbitals with posterior vertical process extending posterior to nasal; frontal posteriorly notched to accommodate an anterior process/bulge of the parietal; maxilla with tall, rounded, wide posterior plate, posterior margin of maxilla anteriorly inclined, gradually increasing in height; maxilla bearing tubercules along ventral border, transverse ridges through rest of the bone; 12 branchiostegal rays, preopercular angle 37.5°, opercular angle 43.8°, subopercular angle 61.4°; anteriorly inclined hyomandibula.

DESCRIPTION

Body Form (Figs 7; 8)

The body is elongate-fusiform and appears rounded in cross section. Specimens are preserved in lateral, dorsal, and ventral views. Median fins are set back on the body, with the dorsal fin originating anterior to the anal fin at scale row 24 and 19 respectively. The caudal fin is heterocercal, deeply cleft, and slightly inequilobate and, like *Wendyichthys dicksoni* (Lund & Poplin, 1997) and *Cyranorhis bergeraci* (Lund & Poplin, 1997), the fin bears an accessory flap on

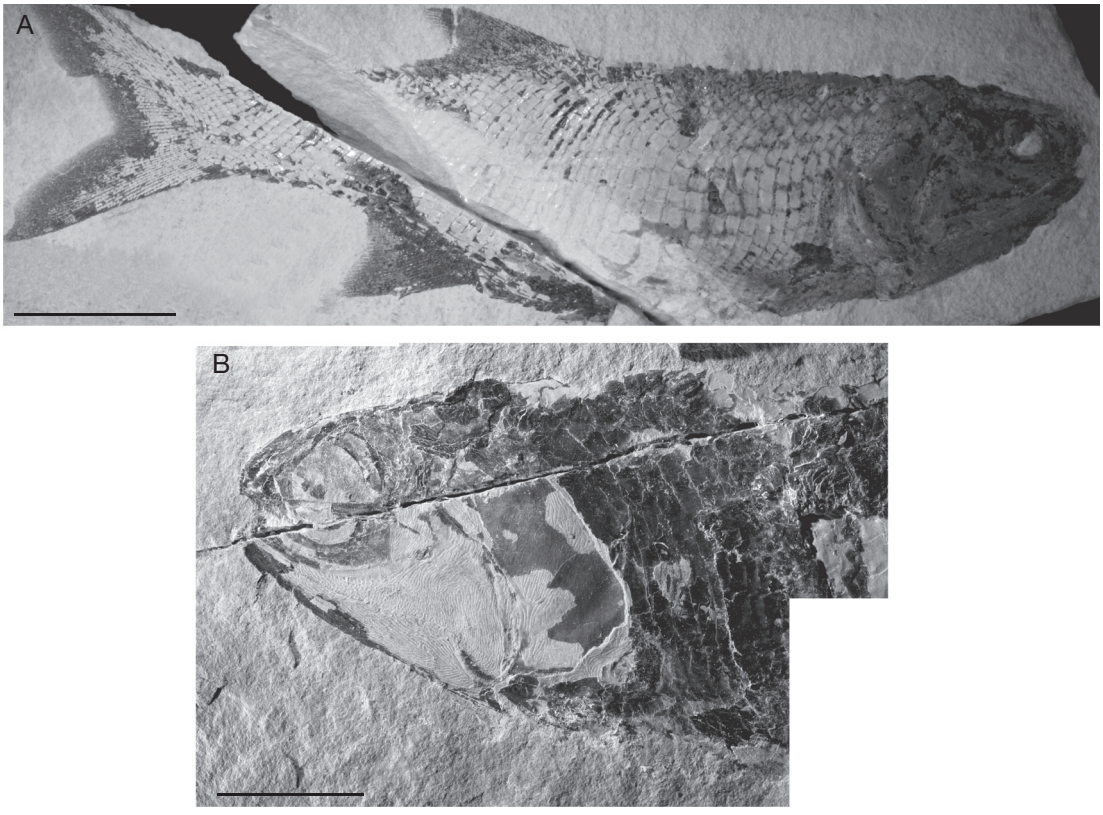

FIG. 7. — *Lineagruan snowyi* n. gen., n. sp.: **A**, MV 2980, left view of the whole fish, natural cast; **B**, holotype (ROM 41809), natural cast of the right lateral view of the head. Scale bars: A, 2 cm; B, 1 cm.

the dorsal lobe (DiCanzio, 1985). Morphometric proportions are listed in Tables 5 and 6.

Snout (Figs 7; 9)

The paired premaxillae each bear two teeth and make up the anterior-most margin of the mouth. They are sutured in the midline and to the ventral margin of the rostropostrostral, and lay anterior to the antorbitals. They are tiny and rhombic with rounded edges. The antorbital is large, with a short vertical portion extending dorsally, ventral to the nasal, and with a horizontal portion extending anteriorly towards the rostropostrostral. It bears a Y-shaped tripartite junction of the supraorbital and infraorbital canals and the ethmoid commissure. The supraorbital canal exits the antorbital and enters the nasal while the ethmoid commissure extends into the rostropostrostral. The nasal is rectangular and situated at an angle due to the placement of the antorbital bones. Posterodorsally, the nasal tapers to a point but does not come in contact with the posterodorsal infraorbital due to the intervention of the frontal. The supraorbital canal can be seen running through the nasal and exiting into the frontal.

Skull roof (Figs 7; 9)

Overall, the skull roof is rather narrow, with the widest portion being at the lateral margin of the dermopterotic. The narrow frontal, bearing the supraorbital canal, widens at the origin of the dermopterotic to produce a posterolateral process. The posterior margin of the frontal is strongly notched to house the parietal. It has a narrow

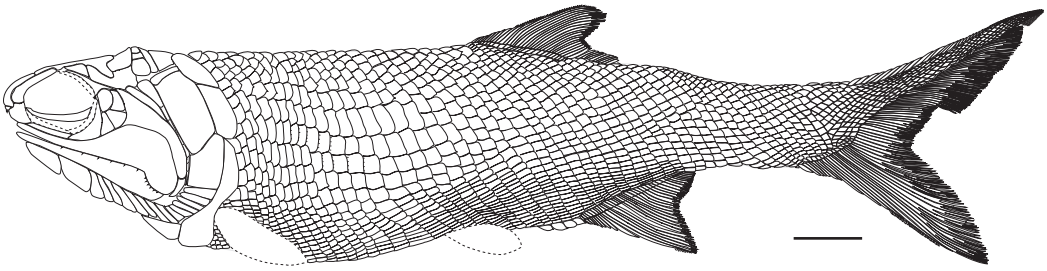

FIG. 8. — *Lineagruan snowyi* n. gen., n. sp., reconstruction based upon MV 2980. Scale bar: 1 cm.

anterior portion, a wide posterolateral process, and a posterior notch.

The parietal is rhombic, anteriorly rounded and slightly spurred at its posterolateral corner. The anterior, middle, and posterior pit lines are not always visible, a result of their posterodorsal placement on the bone. The suture between the parietal and laterally located dermopterotic is hard to determine. The dermosphenotic is located anteriorly, dorsal to the posterodorsal infraorbital, extending anterodorsally to about mid-orbit. It is triangular, lateral to the narrow frontal, and medial to the long expanded arm of the dermopterotic. The majority of the medial margin abuts against the frontal. Posterior to the rectangular arm, the dermopterotic is rounded, spurred ventrally, and notched posteriorly.

Cheek (Figs 7; 9)

Three infraorbitals are present – posterodorsal, posteroventral, and ventral. The posterodorsal infraorbital is a T-shaped bone that makes up the posterodorsal margin of the orbit. Its dorsal arm is longer than the ventral arm, abuts against the dermopterotic, and extends posteriorly to the level of the dorsal tip of the preoperculum. The curve created by the branched arms of the posterodorsal infraorbital holds the spiracular bone. Anteriorly, the posterodorsal infraorbital tapers to a point. The posteroventral infraorbital is crescent-shaped, with the dorsal tip extending towards the ventral arm of the posterodorsal infraorbital. The infraorbital canal bears radiating pore canals in this bone. The first infraorbital is present ventral to the orbit as a narrow band of bone.

Three wedge-shaped suborbitals are present – they are wider posteriorly than anteriorly. The posterior edges are rounded while the anterior edges are squared off. Two large suborbitals fit within the curve of the preoperculum while a third, smaller suborbital is inserted between the maxilla and the posteroventral infraorbital.

Four thinly ossified sclerotics are present.

The preoperculum is hatchet-shaped with a narrow posterior arm and an expanded, curved anterior portion. The preopercular canal runs up the vertical arm and extends into the dorsal arm of the preoperculum. The preopercular pit line is short and can be seen in the narrow arm of the preoperculum. The mean preopercular angle is 37.5°. The dermohyal is a long, narrow, rectangular bone between the anteopercular series and the preoperculum. The dermohyal extends ventrally to about half the height of the operculum. The dorsal margin of the dermohyal abuts against the lateral margin of the dermopterotic.

At least three, thin, delicate, narrow rectangular anteopercular bones are situated along the anterior edge of the subopercular, and there is evidence that additional bones lined the anterior border of the operculum as well. Though they are thin, ganoine ridges can be seen upon them.

The maxilla is long with a tall, wide, rounded posterior plate and a strong posteroventral process. The posterior margin of the maxilla is inclined and gradually increases in height. The narrow anterior process of the maxilla extends ventral to the orbit. The oral margin of the maxilla is toothed along its entire length with two rows of acrodont, conical, anteriorly inclined teeth. The medial teeth are larger than the

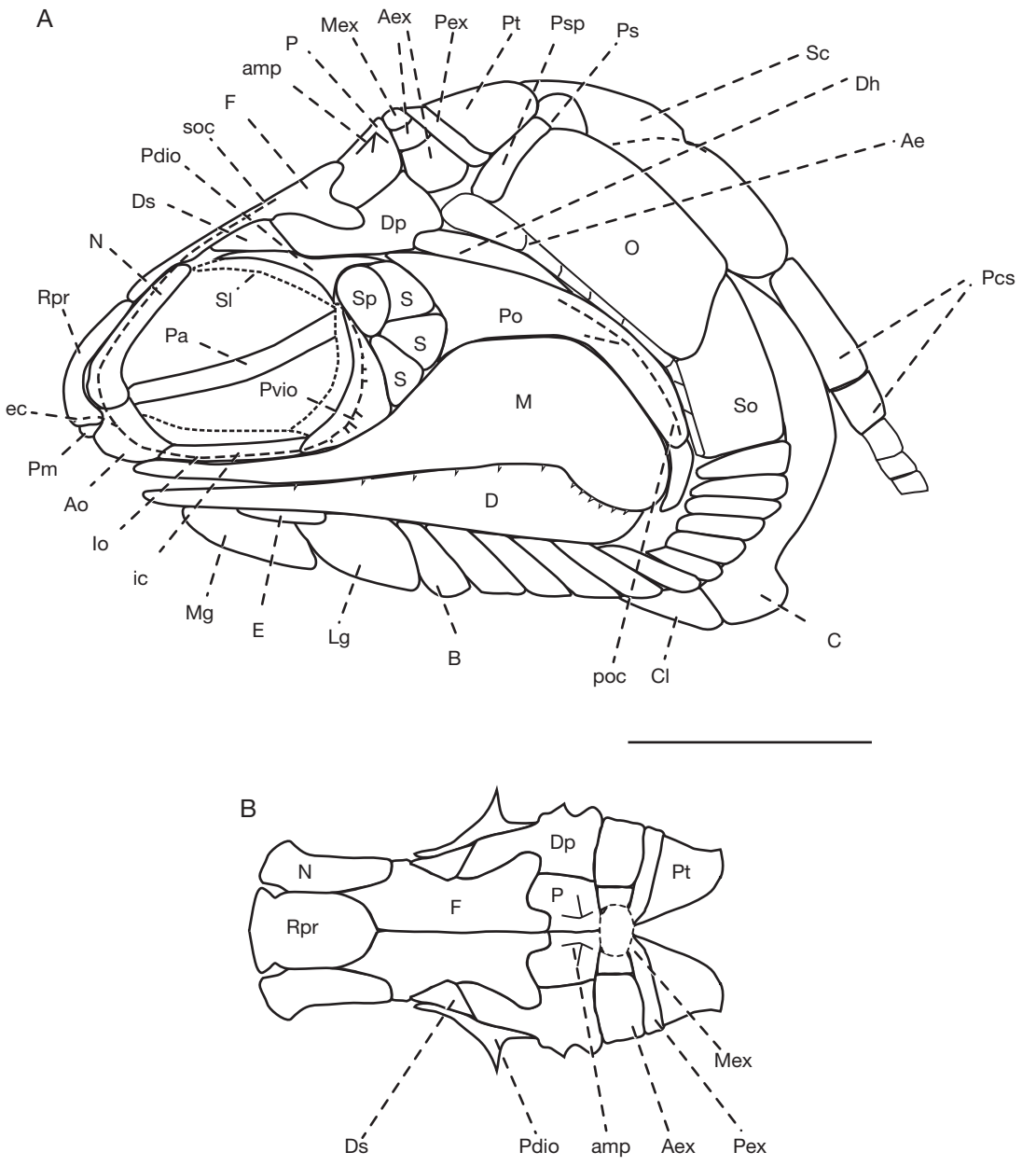

FIG. 9. — *Lineagruan snowyi* n. sp.: **A**, reconstruction of the head in lateral view based upon holotype (ROM 41809 A, B) and MV 2980 A, B; **B**, reconstruction of the dorsal view of the head based upon holotype (ROM 41809 A, B) and MV 2980 A, B. Abbreviations: see Figure 4; **Io**, infraorbital; **Sc**, supracleithrum. Ganoine ornamentation not illustrated because of its preservation. Scale bar: 1 cm.

small lateral teeth. These teeth continue down the length of the posteroventral process. The dentary is entirely toothed with acrodont, conical teeth. The dentary itself is wider posteriorly than anteriorly. The posteroventral process of the maxilla covers a portion of the dentary posteriorly.

Operculo-gular apparatus (Figs 6B; 7; 9)
The operculum is roughly rectangular, situated at an angle of 43.8°. Its ventral margin is curved while the dorsal margin is rounded and slightly narrower than the ventral one. It is shorter posteriorly, increasing in height anteriorly due to the shape of the ventrally located suboperculum. A postspiracular is present as a narrow rectangular bone sutured to the operculum along its dorsal edge. The suboperculum is roughly rectangular, but its dorsal margin is concave in respect to the operculum. The mean subopercular angle is 61.4°.

Twelve branchiostegal rays are seen in lateral view, beginning about half way down the dentary and extending ventral to the suboperculum. Below the dentary, there are narrow, long, rectangular rays. The rays decrease in length at the mandibular corner, only to lengthen again posteriorly. The first branchiostegal ray ventral to the suboperculum is about twice as wide as the other rays. Above the mandibular corner there are three rays while at and below the mandibular corner there are nine. There is a large, paired, rounded lateral gular, one elliptical median gular, and a pair of extralateral gulars. The median and lateral gulars extend along the anterior half of the dentary (Fig. 6B).

Pectoral girdle (Figs 7; 9)
Lineagruan snowyi n. sp. has two sets of paired extrascapulars. The anterior set is the larger and is present as a row of block-like bones posterior to the parietal. This row is composed of two or three lateral and a single median bones. The lateral-most bone is expanded laterally. The posterior extrascapular is a smaller, rectangular bone bearing the supratemporal commissure.

In lateral view, the posttemporal is rounded and acuminate. It is located dorsal to the supracleithrum and posterior to the posterior extrascapular. The supracleithrum is a wide, elliptical bone that is approximately the height of the operculum and overlapped by it so that only the posterior edge of the supracleithrum is exposed. Posteriorly, the supracleithrum is notched about mid-height for the exit of the trunk lateral line canal. The posterior portion of the presupracleithrum is visible posterior to the operculum and anterior to the supracleithrum. The trunk lateral line enters the presupracleithrum and the supracleithrum. The cleithrum is difficult to visualize because it is often covered by the operculum, suboperculum, and branchiostegal rays, but a faint outline can be seen. It appears to taper to a blunt point dorsally, ventral to the supracleithrum. The clavicle is narrow and triangular.

Suspensorium
The hyomandibula is apparent in MV 7010B. It originates at the level of the skull roof posterior to the preoperculum. It is situated at an oblique angle, similar to the angle of the preoperculum.

Squamation (Fig. 9)
There is one row of rectangular postcleithral scales that bear circumferential ridges and are not pectinated. The flank scales are rectangular, bear longitudinal ridges, and have pectinated posterior margins. The ventral mid body scales are narrow and rectangular. There is a noticeable scale row inversion at scale row 48-49.

Fins
The pectoral fin has thin, delicate rays but it is unclear if it bore fringing fulcra. The small pelvic fin is roughly rectangular, consists of long, thin, highly segmented, and distally branched rays, and bears short fine fringing fulcra on its anterior edge.

The dorsal and anal fins are triangular, with thin, highly segmented and distally branched fin rays. The dorsal fin originates anterior to the origin of the anal fin. Both dorsal and anal fin bases are composed of rectangular guard scales and short basal fulcra form the leading edges. Posterior to the basal fulcra, the leading edges of both the dorsal and anal fins are lined with short fringing fulcra. Posteriorly, the dorsal fin rays taper off gradually, creating a trailing end of short fin rays. The posterior tapered portion of the anal fin is not as long as that of the dorsal fin. There are at least four rounded, acuminate predorsal ridge scales.

The heterocercal caudal fin is deeply forked and slightly inequilobate. The rays that make up the caudal fin are narrow, delicate, highly segmented, and branched distally. At least four ridge scales are seen anterior to the ventral lobe of the caudal fin.

Posterior to the precaudal ventral ridge scales, the ventral lobe is lined with closely packed, short, stout fringing fulcra. Anterior to the epicaudal lobe of the caudal fin, at least four ridge scales are present. Posterior to the precaudal dorsal ridge scales, the anterior half of the caudal fin bears long, thin, overlapping basal fulcra that decrease in size posteriorly. Posteriorly, the epicaudal lobe bears shorter fringing fulcra.

Genus *Beagiascus* n. gen.

TYPE AND ONLY SPECIES. — *Beagiascus pulcherrimus* n. sp.

ETYMOLOGY. — *Beagiascus*, from *beag*, Gaelic for few and rare, *iasc*, fish,

Beagiascus pulcherrimus n. sp.
(Figs 10-12; Tables 9-12)

ETYMOLOGY. — *Pulcher*, Latin for beautiful.

HOLOTYPE. — CM 35349.

REFERRED SPECIMENS. — CM 35350, CM 46121, CM 48529, CM 63061, CM 63076, CM 78511, CM 78512; MV 2551, MV 2930, MV 3801, MV 3806, ROM 29769, ROM 43840, ROM 43982.

OCCURRENCE. — Upper Mississippian (Serpukhovian, Namurian E2b) Bear Gulch Limestone lens, Bear Gulch Limestone Member of the Heath Formation, Big Snowy Group, southwest of Becket, Fergus County, Montana (USA).

DIAGNOSIS. — A lower actinopterygian fish defined by the following combination of characters: elongate fusiform body, narrow in cross section; premaxillae narrowly sutured in midline; nasal notched anteriorly and posteriorly; posterodorsal process of antorbital forms base of posterior nasal notch; frontal with a sinuous sagittal suture; crescent-shaped dermosphenotic; large dermopterotic with a wide posterior plate, laterally spurred, anteromedial process situated within a notch in the frontal; three large suborbitals situated within curve of preoperculum, small fourth suborbital overlapping large suborbital, suborbital between posteroventral infraorbital and maxilla; four infraorbitals – narrow infraorbital ventral to orbit, crescent-shaped posteroventral infraorbital, an intervening element, and T-shaped posterodorsal infraorbital, tapered anterior end of posterodorsal infraorbital comes in contact with tapered posterior end of nasal; mosaic of several small bones in curve of posterodorsal infraorbital for spiracular bone; long maxillary plate; two rows of pointed, posteriorly inclined teeth down length of maxilla; prominent posteroventral process of maxilla; anteriorly inclined hatchet shaped preoperculum; one row of 5 or 6 anteopercular bones along anterior margin of operculum – ventral-most anteopercular bone wider and longer than the others; rectangular, anteriorly inclined operculum with transverse ganoine ridges; rhombic suboperculum with vertical ganoine ridges; total of 14 or 15 branchiostegal rays – five above mandibular corner, 9 or 10 at and below mandibular corner, first branchiostegal twice as high as second; anterior and posterior extrascapular rows sharing median extrascapular (anterior row – three lateral bones, posterior-single bone bearing supratemporal commissure); unsutured postspiracular; one row of rhombic postcleithral scales; narrow ventrolateral flank scales; flank scales finely pectinated; fan-like pectoral fin; triangular pelvic fin, triangular dorsal and anal fins with posterior edges tapering off gradually; heterocercal caudal fin deeply forked, accessory flap on epicaudal lobe; all fins bear long, stout, overlapping fringing fulcra on leading edges; precaudal ridge scales continuous between the anal and caudal, and dorsal and caudal fins. Meristic, morphometric, and cranial measurements are presented in Tables 9 to 12.

DESCRIPTION

Body form (Figs 10; 11)

The body shape is elongate-fusiform and, because all fish are preserved in lateral view, is likely to have been relatively compressed. The snout of *B. pulcherrimus* n. sp. is blunt and rounded relative to the subterminal mouth. The median fins are set back on the body, with the dorsal fin origin above that of the anal fin. Meristic and morphometric data are found in Tables 9 and 10.

Snout (Figs 10; 12)

The premaxillae are easily seen in lateral view due to their placement and size. They are paired wedge-shaped bones that flank the rostropostrostral and appear to sit within a curve on the ventral margin of the latter. The ventral margin of the rostropostrostral virtually separates the premaxillae, causing these two bones to be sutured narrowly in the midline. The premaxillae contribute to the margin of the mouth and are toothed.

The antorbital is principally located ventral to the nasal bone and extends anteriorly towards the

TABLE 9. — *Beagiascus pulcherrimus* n. gen., n. sp., meristics counts. Abbreviations: see Table 1.

	DFP	AFP	CFP	P2P	NP1	NP2	SBL	SAL	NDOR	NAN	NCAU
Mean	38	29	63	17	17	19	17	14	52	49	101
Min	34	26	58	14	14	16	11	14	46	41	82
Max	39	33	71	20	22	20	11	14	57	57	112
N	8	9	7	3	9	4	1	1	6	6	3
ST DEV	1.75	2.54	4.45	3	2.67	1.89	–	–	5.35	6.63	16.77

TABLE 10. — *Beagiascus pulcherrimus* n. gen., n. sp., natural logarithms of morphometric measurements (in cm). Abbreviations: see Table 2.

	ABAS	AOCV	CBAS	CPL	CPW	DBAS	DOCD	FORK	HTDO	MXHT	P1P2	P2AO	SAO	SDO	SL	SP1	SP2
Mean	0.77	1.22	1.31	0.33	0.08	0.76	1.35	2.57	0.96	1.08	1.00	0.55	1.97	1.95	2.44	1.07	1.74
Min	0.64	1.13	0.99	-0.11	-0.11	0.41	1.19	2.50	0.79	0.92	0.41	0	1.74	1.79	2.24	0.88	1.44
Max	0.88	1.36	1.41	1.06	0.34	0.99	1.48	2.62	1.1	1.34	1.39	0.79	2.1	2.05	2.56	1.22	1.99
N	8	8	7	9	9	8	9	7	9	8	5	5	9	9	9	8	6
ST DEV	0.09	0.10	0.15	0.36	0.17	0.18	0.12	0.05	0.10	0.16	0.36	0.32	0.13	0.08	0.10	0.14	0.19

TABLE 11. — Cranial measurements for *Beagiascus pulcherrimus* n. gen., n. sp., natural logarithms of cranial triangle and individual bone measurements (in mm). Abbreviations: see Table 3.

	BCL	B1H	IOQ	MH	ML	MPL	OH	OW	PH	SH	SIO	IOSK	SKQ	SQ
Mean	3.07	0.56	2.57	1.64	3.03	2.02	2.31	1.49	1.57	1.45	2.71	2.15	2.74	3.26
Min	2.93	0.34	2.43	1.29	2.90	1.63	2.24	1.38	1.31	1.00	2.60	2.04	2.60	3.12
Max	3.15	0.71	2.67	1.93	3.20	2.31	2.40	1.58	1.78	1.72	2.80	2.25	2.84	3.36
N	7	5	6	7	7	7	7	7	7	7	6	6	6	6
ST DEV	0.08	0.15	0.08	0.25	0.11	0.22	0.06	0.08	0.16	0.25	0.09	0.08	0.09	0.10

TABLE 12. — Cranial measurements for *Beagiascus pulcherrimus* n. gen., n. sp., cranial angles. Abbreviations: see Table 4.

	K	OA	Pp	Q	Sn	SA
Mean	88.04	41.40	39.40	55.96	36.04	70.97
Min	72.16	31.11	35.00	66.35	30.87	51.13
Max	95.43	52.78	47.52	50.33	41.50	85.19
N	6	7	7	6	6	6
ST DEV	9.11	8.67	5.04	5.89	3.73	12.50

rostropostrostral. Posteriorly, a dorsal process of the antorbital extends posterior to the ventral margin of the nasal and contributes to the anterior portion of the orbit. The antorbital bears a Y-shaped branching canal formed by the junction of the supraorbital canal, infraorbital canal, and ethmoid commissure. The supraorbital canal can be traced into the nasal, while the ethmoid commissure extends anteriorly into the rostropostrostral.

The nasal is tall, narrow, notched anteroventrally, and tapers to a point as it extends dorsally towards the skull roof. The anteroventral notch is complimentary to the rostropostrostral notch, thus forming the anterior nasal opening. The posterior nasal notch is bordered by the antorbital, thus supporting the continuation of the supraorbital canal from the antorbital to the frontal. Posteriorly, the nasal is in contact with the posterodorsal infraorbital.

A large unpaired rostropostrostral bears the ethmoid commissure ventrally and extends dorsally to abut against the frontals. Ventrally, it comes close to separating the paired premaxillae in the midline. The rostropostrostral is notched ventrolaterally, and thereby contributes to forming the anterior nasal opening.

Skull roof (Figs 10; 12)

The skull roof is narrow above the orbit and gradually expands to its widest point at the posterolateral

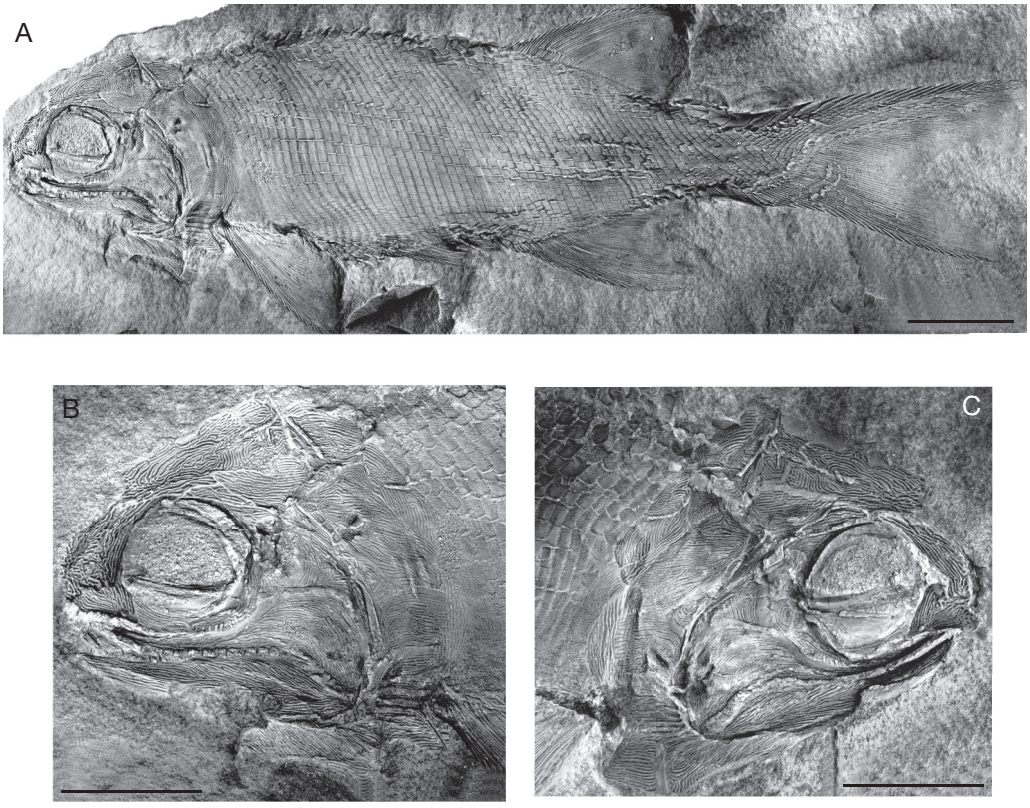

FIG. 10. — *Beagiascus pulcherrimus* n. gen., n. sp., holotype (CM 35349): **A**, left side of the whole fish, natural cast; **B**, left lateral view of the head; **C**, right lateral view of the head. Specimens shadowed with magnesium oxide. Scale bars: 1 cm.

corner of the dermopterotic. The dorsal margin of the orbit is bound by the posterodorsal infraorbital and nasal; no supraorbitals are present. The lateral margin of the frontal is deeply notched to accommodate the anterior process of the dermopterotic. A small lateral spur is found anterior to the notch (MV 2551) at the point where the posterodorsal infraorbital comes in contact with the nasal. Posterior to the notch, the frontal gradually flares out, becoming wider and round. The paired frontals join in a raggedly sinuous sagittal suture.

The paired parietals are rhombic, approximately ⅙ the length of the frontals, and each bear the anterior, middle, and posterior pit lines. The lateral margin of the parietal is somewhat angled, creating an oblique suture between the parietal and the dermopterotic. The dermosphenotic is a crescent-shaped bone located medially to the posterodorsal infraorbital and lateral to the frontal. The length of the dermosphenotic is 0.69 times that of the dermopterotic. In at least one specimen, CM35349, the infraorbital canal can be seen along the lateral border of the dermosphenotic. The dermopterotic is a large bone located laterally to the frontal and parietal, posterior to the posterodorsal infraorbital. Posteriorly, it has a tall plate-like process with a rather straight margin lateral to the parietal bone. Anterior to this plate, the dermopterotic is curved and is situated close to the portion of the frontal that flares out. The anteromedial portion of the dermopterotic tapers to a point that is situated within a notch on the frontal. Laterally, the dermopterotic is spurred at the posterior margin of the posterodorsal infraorbital. The posterolateral corner of the dermopterotic is rounded while the

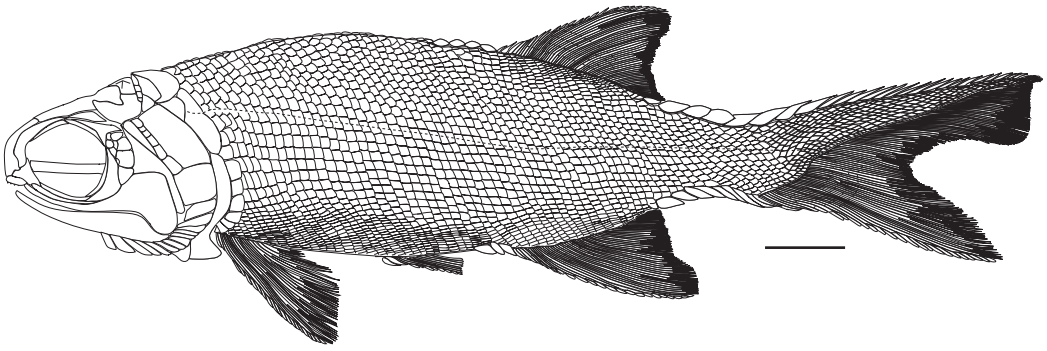

FIG. 11. — *Beagiascus pulcherrimus* n. gen., n. sp., reconstruction based upon holotype (CM 35349). Scale bar: 1 cm.

posteromedial corner is notched at about the level of the anterior extrascapulars.

Cheek (Figs 10; 12)

Three infraorbitals are present. The first is narrow and located ventral to the orbit. The second, the posteroventral infraorbital, is roughly crescent-shaped, but has a slightly concave posterior border. It bears the infraorbital canal, which has distinct radiating pore canals extending towards the posterior border of the bone. The third, the posterodorsal infraorbital, is T-shaped and comes in contact with the tapered posterior point of the nasal bone.

There are three large suborbitals that primarily sit within the anterior curve of the preoperculum. The posterior edges of the suborbitals appear to overlap with the ganoine-free anterior edge of the preoperculum. The ventral-most suborbital is inserted between the maxilla and the posteroventral infraorbital. A much smaller fourth suborbital is located posterior to the posteroventral infraorbital. Dorsal to the three large suborbitals is a mosaic of several small round spiracular bones that lie primarily within the curved posterior arm of the posterodorsal infraorbital. Individual bones cannot be confidently counted; a result of the poor preservation of this area.

The preoperculum is tall and hatchet-shaped – the average angle between the two limbs is 39.4°. The preopercular canal can be traced from the narrow vertical arm up into the dorsal process. A pit line is seen in the dorsal region of the bone. Collectively, the pit line and the preopercular canal are Y-shaped.

The maxilla is long with a tall, rounded, posterior plate. Anteriorly, the maxilla tapers to form a narrow process that runs ventral to the orbit. Rows of large and small acrodont teeth are present down the length of the maxilla. The tips of the large teeth are recurved and angled posteriorly. The ventral margin of the maxilla is relatively straight while the dorsal margin is curved under the orbit. Posteriorly, near the maxillary fossa, the posteroventral process of the maxilla bears long, narrow teeth. These teeth, unlike those found down the length of the maxilla, are angled anteriorly. Large teeth are found along the entire length of the dentary.

The dermohyal is wedge-shaped and situated between the preoperculum and anteopercular bones. It extends ventrally to about half the length of the operculum.

The 5 or 6 anteopercular bones run along the height of the anterior margin of the operculum, posterior to the preoperculum and dermohyal. The ventral-most bone is ventrally expanded, making it longer and wider than the dorsal bones. In one specimen, CM 48529, a second anteopercular row composed of two additional block-shaped bones appears to be present at the level of the subopercular.

Operculo-gular apparatus (Figs 10; 12)

The operculum is situated at an angle of 41.4°. It is roughly rectangular with a width that is about half

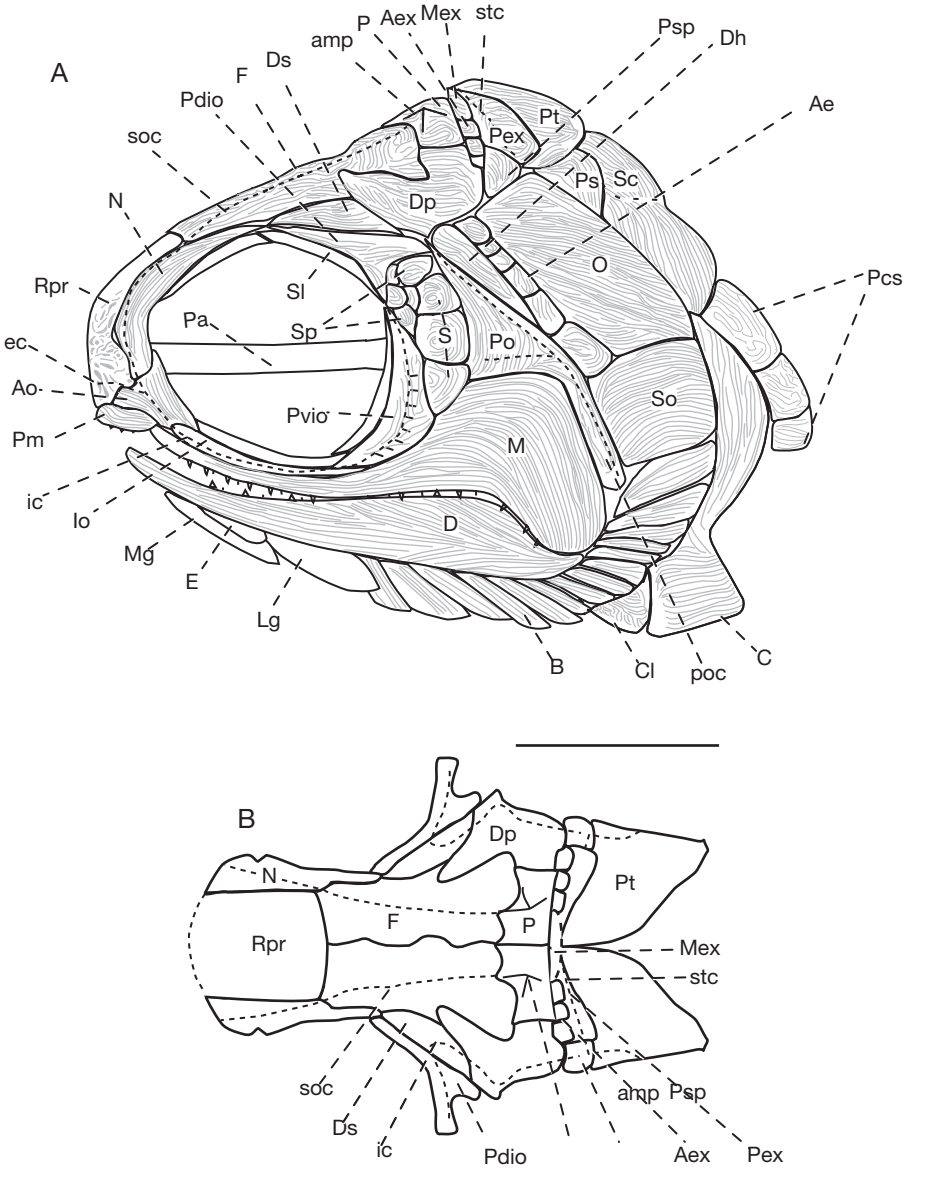

FIG. 12. — *Beagiascus pulcherrimus* n. gen., n. sp.: **A**, reconstruction of the head in lateral view based upon holotype (CM 35349 A, B), MV 2551 A, and CM 48529; **B**, reconstruction of the head in dorsal view based upon holotype (CM 35349 A, B), MV 2551 A, B, and CM 48529. Abbreviations: see Figure 4. Scale bar: 1 cm.

its height. The rhombic suboperculum is about half the height of the operculum, but approximately as wide, and has a convex upper suture.

A rounded postspiracular is present dorsal to the operculum and ventral to the anterior and posterior extrascapulars. The postspiracular is not sutured to the operculum.

In lateral view, the series of 14 or 15 branchiostegal rays extends from the suboperculum to about the middle of the ventral margin of the dentary.

Above the mandibular corner there are five rays, below there are 9 or 10. The first branchiostegal ray is wider and longer than the other rays in the series and is roughly half the height of the suboperculum. Rays at the level of the pectoral notch in the cleithrum are short – anterior to this notch, the rays are longer.

A large median gular, a pair of extralateral gulars, and a pair of lateral gulars are present.

Pectoral girdle (Figs 10; 12)

An anterior and a posterior row of extrascapulars are present. The anterior extrascapulars are present as a row of three lateral, and one median blocks. The posterior extrascapulars are rectangular bands of bones that originate at the median extrascapular. In one specimen, CM 35349, the supratemporal commissure seems to be located between the two sets of extrascapulars, with the radiating pore canals entering through the posterior extrascapular.

The posttemporal appears round and acuminate in lateral view, but in the dorsal view, the bone appears rectangular with a curved lateral margin. A presupracleithrum is present as a rounded bone posterior to the operculum and anterior to the supracleithrum. The anterior margin is covered by the operculum. The dorsal margin of the presupracleithrum has a narrow rectangular strip of bone that is lacking any ganoine pattern and appears to be spurred in the posterodorsal and posteroventral corners. When all of the dermal bones are in place, these spurs would be internal to the other bones. Likewise, the narrow ganoine-free portion of the presupracleithrum is not visible when all bones are *in situ*. This section of the presupracleithrum may act as a flange to fix the presupracleithrum to the supracleithrum. The supracleithrum is roughly elliptical. The posterior margin of the bone is notched for the exit of the trunk lateral line canal at around the midpoint of the bone. The supracleithrum is as long as the operculum, overlaps and covers the anterior portion of the cleithrum.

The cleithrum extends dorsally to about the dorsal border of the suboperculum. Ventrally, it is deeply notched to hold the pectoral fin. Beyond the notch, the cleithrum continues ventrally, flaring out under the branchiostegal rays at the mandibular corner. A clavicle is visible in lateral view as a triangular bone located mesial and posterior to the branchiostegal rays and anterior to the cleithrum.

Sclerotics

The sclerotic bones are crescent-shaped with their anterior and posterior tips overlapping each other. The ventral and posterodorsal sclerotics are substantial bones that are heavily ossified and clearly seen in numerous specimens. Other sclerotics are not always seen, suggesting they are thinner, less ossified bones, but one specimen, MV 2930, has four crescent-shaped sclerotics.

Palate

The palate is disturbed and inverted in MV 2930 so that the ventral side is visible in the orbit. The palate is heavily toothed with a large patch of pointed teeth. It is closely situated to the parasphenoid.

Squamation (Fig. 12)

There is one row of large block-shaped postcleithral scales. Flank scales are rectangular and finely pectinated. Ventral abdominal scales are narrow rectangles.

Fins

The pectoral and pelvic fins have heavy fringing fulcra on their leading edges. The rays are thin, segmented and have limited delicate distal branches. The pectoral fins are large and fan-like with a mean of 22 rays. The triangular pelvic fins have a mean of 15 rays.

The dorsal fin is situated slightly anterior to the anal fin. Both the dorsal and anal fins are triangular with posterior edges that gradually decrease in size. Anterior to the dorsal fin, 4 or 5 rounded, acuminate ridge scales are seen on the dorsal border of the body. Posterior to the ridge scales, 4 or 5 short, basal fulcra form the leading edge of the fin. The mean dorsal and anal fin ray counts are 51 and 47 rays, respectively. Both median fins have strong fringing fulcra on the dorsal-most edge of the fin. The leading edge of the anal fin is also formed by 4 or 5 short basal fulcra, but it appears that there are no ridge scales anterior to the anal fin. Both median fins have strong fringing fulcra on the dorsal and

ventral-most edge of the fin and thin, jointed rays that are delicately divided distally.

The caudal fin also bears fringing fulcra on the edges of the dorsal and ventral lobes, as well as anteriorly placed ridge scales. The dorsal and ventral margins of the caudal peduncle are lined by oval overlapping ridge scales that appear more rectangular posteriorly. Dorsally, 6 or 7 ridge scales extend from the posterior margin of the dorsal fin to the dorsal lobe of the caudal fin. Ventrally, at least 4-6 ridge scales are seen. The caudal fin is heterocercal, deeply forked and has a dorsal lobe with an accessory flap, giving the dorsal lobe of the caudal fin a notched appearance.

DISCUSSION

Intraspecific Variation in *Lineagruan judithi* n. gen., n. sp.

Lineagruan judithi n. gen., n. sp. is characterized by bilateral asymmetry of numerous cranial bones within individuals in addition to intraspecific variation. For example, the extrascapulars vary between the left and right sides of certain specimens, as well as among specimens. The most common condition is to have anterior and posterior rows of extrascapulars on both sides, separated by a median extrascapular (MV 6372, CM 46283, CM 48768, CM 35596, MV 6132, CM 36592, CM 48765, CM 35595, and CM 35412). Within this condition, variants are seen. The number of anterior extrascapulars of left and right sides varies from 2 or 3 within specimens as well as among different specimens. Another condition is seen in CM 48768, which bears a single row of four lateral extrascapulars separated by a median extrascapular – the posterior extrascapular row is not present.

Variation is also seen in the condition of the operculum and subopercula (Fig. 5). While the majority of the specimens of *L. judithi* n. gen., n. sp. have separate opercula and subopercula, they are fused in two specimens with well ossified braincases (CM 35412, CM 63078). This fusion would have ensured that the operculum and subopercula acted as a single functional unit. Both the fused and unfused bones bear vertical ridges of ganoine – suggesting that even if there were individual bones, each were subjected to similar stresses and may have functioned as if they were a unit (Lund & Younan 1994). The cause of the fusion of these bones is unknown.

The extent of the anteopercular bones is another source of variation. The majority of the specimens that have anteopercular bones show a condition where the anteopercular bones extend to the ventral margin of the operculum. The exception to this condition is seen in one specimen, CM 63078, which shows the anteopercular bones extending to the ventral margin of the subopercula. This specimen also has the operculum and subopercula fused, further supporting the idea that these two bones worked "in unison".

Morphometric differences

Meristic data illustrate separation of *Lineagruan judithi* n. gen., n. sp., *L. snowyi* n. gen., n. sp., and *Beagiascus pulcherrimus* n. gen., n. sp. on the basis of combinations of standard length, caudal peduncle length, and snout to dorsal origin length (Fig. 13; Tables 1; 2; 5; 6; 9; 10). *Lineagruan judithi* n. gen., n. sp. appears to be characterized by a smaller total body length relative to *L. snowyi* n. gen., n. sp. and *B. pulcherrimus* n. gen., n. sp. – apparently a result of a shortening of the head and caudal peduncle. Differences are also seen in the base length of all median and caudal fins – with larger fin base lengths seen in *L. snowyi* n. gen., n. sp. and *B. pulcherrimus* n. gen., n. sp. than in *L. judithi* n. gen., n. sp. (Tables 1; 2; 5; 6; 9; 10).

Differences in fin ray counts vary with differences in the lengths of fin bases (Tables 1; 2; 5; 6; 9; 10). These are not accounted for by differences in scale numbers. *Beagiascus pulcherrimus* n. gen., n. sp. is characterized by significantly higher fin ray numbers when compared to both *Lineagruan* species, especially in caudal fin ray counts. The packing density of fin rays in *B. pulcherrimus* n. gen., n. sp. is greater than that of the *Lineagruan* species and seems to be related to the fact that the fin rays of the former are much thinner than that of the latter. Morphometric data illustrates differences in fin placement (Tables 1; 2; 5; 6; 9; 10; Fig. 14). Separation between *B. pulcherrimus* n. gen., n. sp. and *Lineagruan* is seen, with

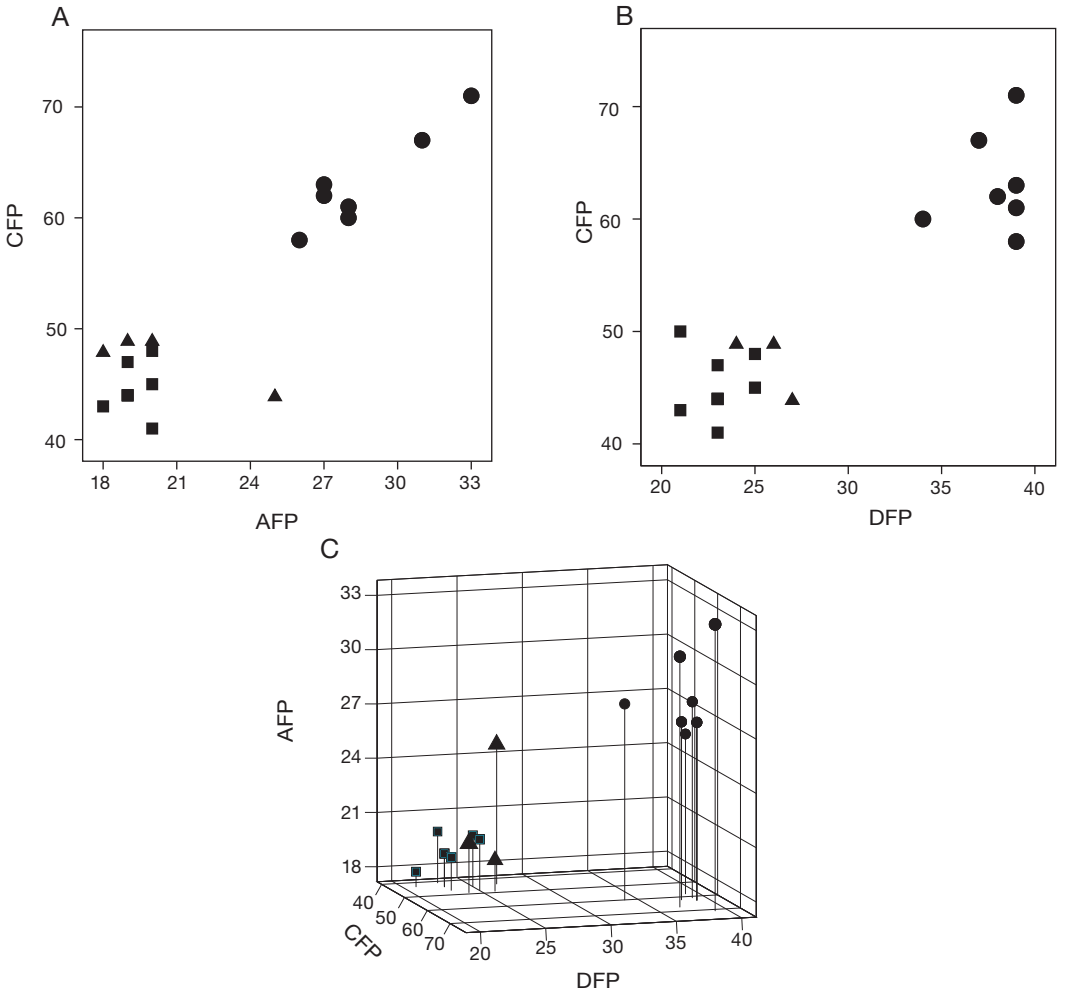

FIG. 13. — Comparisons of meristic counts for *Lineagruan judithi* n. gen., n. sp. (■), *L. snowyi* n. gen., n. sp. (▲), and *Beagiascus pulcherrimus* n. gen., n. sp. (●): **A**, anal fin position (AFP) to caudal fin position (CFP); **B**, dorsal fin position (DFP) to caudal fin position (CFP); **C**, dorsal fin position (DFP) to caudal fin position (CFP) to anal fin position (AFP).

B. pulcherrimus n. gen., n. sp. characterized by an increase in the number of scale rows between the head and the dorsal, anal, and caudal fins.

The most significant difference among the species is seen in cranial dimensions and lengths shown by the cranial triangle measurements and further accentuated by comparison to *Kalops* Poplin & Lund, 2002 (Poplin & Lund 2002; Fig. 15). Principle component analysis extracted two components that account for 93.7% and 6.3% of the variance, respectively, between *Lineagruan judithi* n. gen., n. sp., *L. snowyi* n. gen., n. sp., and *B. pulcherrimus* n. gen., n. sp. Discriminant analysis identified two functions as discriminating between the three taxa. When each of the fishes were plotted against these functions, the three groupings of fish were shown to occupy distinct and separate morphospaces with no overlap (Fig. 14). The classification function in SPSS that "grades" how well the specimens were grouped on the basis of the analyzed variables, determined that 100% of the originally grouped cases were found to be classified correctly. The cranial characteristics

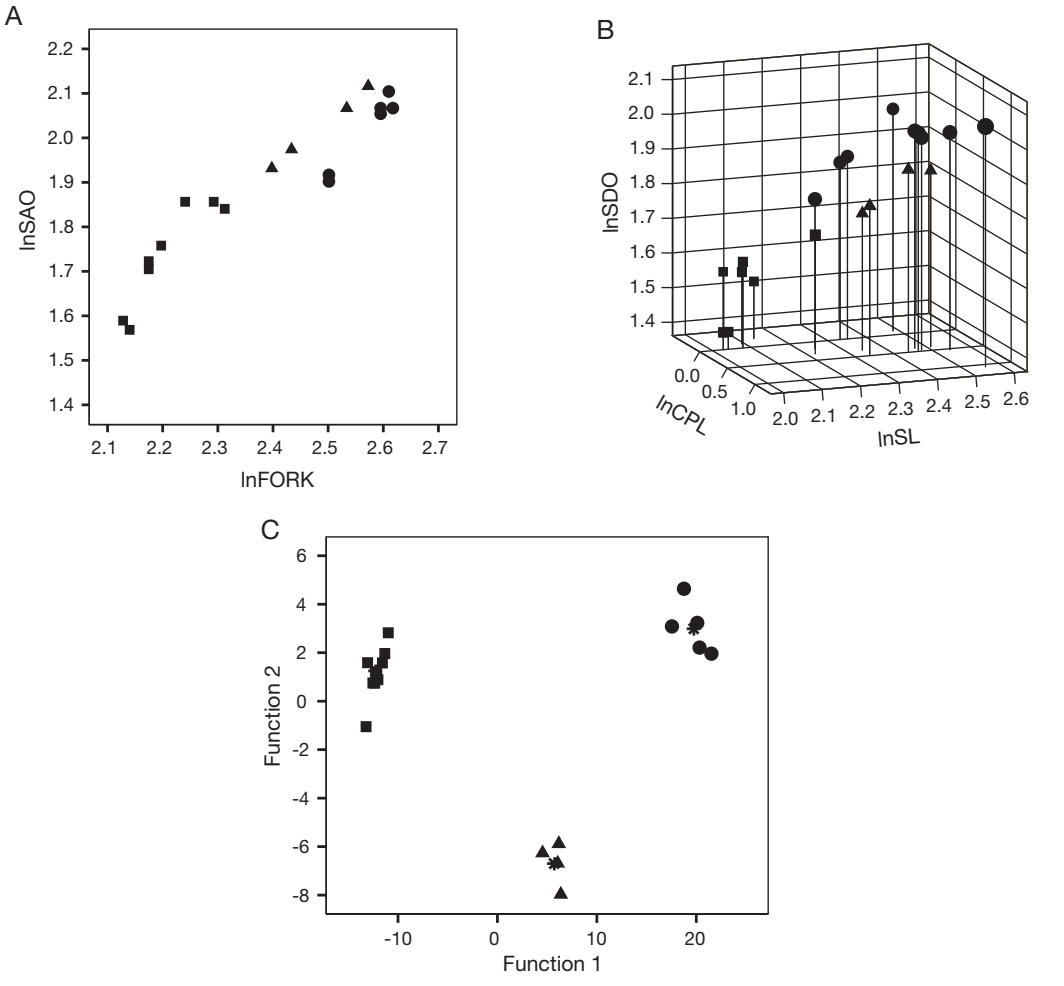

FIG. 14. — Comparisons of morphometric measurements for *Lineagruan judithi* n. gen., n. sp. (■), *L. snowyi* n. gen., n. sp. (▲), and *Beagiascus pulcherrimus* n. gen., n. sp. (●): **A**, natural logs of fork length (lnFORK) to snout-origin of anal fin (lnSAO); **B**, natural logs of standard length (lnSL) to caudal peduncle length (lnCPL) to snout-origin of dorsal fin length (lnSDO); **C**, distinct morphospaces of *L. judithi* n. gen., n. sp., *L. snowyi* n. gen., n. sp., and *B. pulcherrimus* n. gen., n. sp. obtained by plotting each fish for the functions extracted from discriminant analysis of cranial measurements. Function 1, natural logs of SIO, SQ, BCL, SH, OH, IOQ, MH, and PH, accounting for 93.7% of the variance seen between the three groups. Function 2, natural logs of OW, MPL, ML, SKQ, IOSK, accounting for 6.3% of the variance seen. Asterisks represent group centroids. Abbreviations: see Figure 1.

leading to a majority of the variance between the three fishes are described in Figure 15.

Beagiascus pulcherrimus n. gen., n. sp., *Lineagruan judithi* n. gen., n. sp., and *L. snowyi* n. gen., n. sp. display distinct morphological differences shown by the morphometric, meristic, and osteological data. The combinations of variables involved in the morphometric and osteological separation of these species strongly suggest a functional (ecomorphological) component to their differences.

FUNCTIONAL CONSIDERATIONS

Fins and fin rays

Caudal fin heterocercy, an accessory caudal flap, fringing fulcra, and the nature and number of caudal fin rays are features of the three species that

suggest specializations with respect to swimming style, hydrodynamics, and control of fine-scale fin movements.

Fringing fulcra are much smaller elements transitional to the fin rays (Cloutier & Arratia 2004). Fringing fulcra, basal fulcra, and procurrent fin rays are considered to have stiffened the edges of the fins (Gardiner 1984). Though all three fishes possess fringing fulcra, there are differences in the nature of the fulcra between and within the genera. The leading edges of all the fins of *B. pulcherrimus* n. gen., n. sp. are lined with tightly packed stout fringing fulcra, while the fringing fulcra of *Lineagruan* are small and thin. The fringing fulcra of *B. pulcherrimus* n. gen., n. sp. may have allowed for stiffer leading edges of the paired and unpaired fins than either species of *Lineagruan*.

Lineagruan judithi n. gen., n. sp., *L. snowyi* n. gen., n. sp., and *B. pulcherrimus* n. gen., n. sp. possess fine, closely fitted, and jointed fin rays. Those of *Lineagruan judithi* n. gen., n. sp. and *L. snowyi* n. gen., n. sp. (caudal mean of 56, 62 respectively) are relatively stouter and less closely spaced than in *B. pulcherrimus* n. gen., n. sp. (caudal mean 101) and the latter exhibits multiple distal bifurcations of the rays. The highly flexible fin rays may allow for a fish to actively control the force produced by the tail while maneuvering (Videler 1996; Liao & Lauder 2000). The close packing and fine nature of these fin rays may have had a functional significance, e.g., fine-scale control of fin flexibility or stiffness. Distal bifurcation of such rays may also impact the fine scale ability to maneuver.

While the fine fin rays may have provided a caudal fin capable of improved maneuverability, the presence of several ridge scales immediately anterior to the caudal in *L. judithi* n. gen., n. sp. and *L. snowyi* n. gen., n. sp., plus the long dorsal caudal fulcra, may have stiffened the caudal peduncle and the dorsal lobe of the fin – aiding in acceleration (Videler 1996). *Beagiascus pulcherrimus* n. gen., n. sp., on the other hand is characterized by continuous rows of dorsal and ventral ridge scales between the caudal and both the dorsal and anal fins, respectively. These continuous ridge scales may have stiffened the entire caudal region of the fish rather than the caudal peduncle alone. The caudal fulcra may have additionally provided a caudal fin support mechanism analogous to the skeletal uroneural elements of lower teleosts (Schultze & Arratia 1989).

Both species of *Lineagruan* as well as *Beagiascus pulcherrimus* n. gen., n. sp. possess an accessory flap, a posterior extension of the upper rays of the dorsal lobe of the caudal fin. This trait is also seen in *Wendyichthys dicksoni* (Lund & Poplin 1997) and *Cyranorhis bergeraci* (Di Canzio 1985; Lund & Poplin 1997). An accessory caudal flap is not seen in recent bony fishes, but is common among recent sharks. Ferry & Lauder (1996) found that the enlarged terminal lobe is vital in the functioning of the caudal fin. However, gross morphological similarities do not necessarily lead to functional similarities. Just as there are kinematic differences between the heterocercal fin of sharks and that of the sturgeon (Liao & Lauder 2000; Wilga & Lauder 2002), there are also likely to be functional differences between the accessory caudal flap of today's sharks and the Paleozoic paleoniscoids.

Feeding and respiration

Respiration in bony fishes is reliant on pressure differences created by changing the volume of the buccal cavity anterior to the gills, and the opercular cavity posterior to the gills (Helfman *et al.* 1997; Liem *et al.* 2001). The suction created by the expansion of the buccal cavity aids in pulling prey located in front of the fish into the mouth. All three fishes examined in this study – as well as two other Bear Gulch palaeoniscoids, *W. dicksoni* and *C. bergeraci* are characterized by the presence of extralateral gulars (Lund & Poplin 1997). Though these bones are not often seen among palaeoniscoids, it cannot be determined if this is due to these bones being an actual rarity or preservational issues (Lund & Poplin 1997). Clear ventral views of extended gulars and branchiostegals of palaeoniscoids can be rare, making it difficult to determine if these narrow bones are present.

Lund & Poplin (1997) presented three interpretations on the nature of extralateral gulars. The favored interpretation proposed that extralateral gulars are mechanical adaptations that allow for a greater widening of the oral-branchial cavity during respiration and feeding. This would be similar to

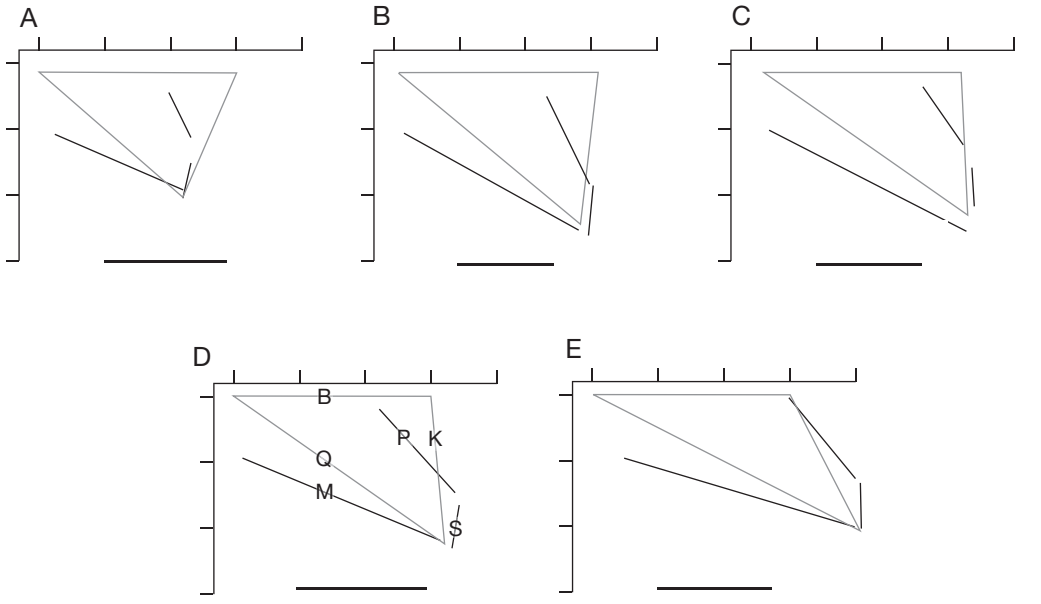

FIG. 15. — Cranial diagrams of some Bear Gulch actinopterygians, scaled to equal braincase lengths: **A**, *Lineagruan judithi* n. gen., n. sp., CM 62743; **B**, *L. snowyi* n. gen., n. sp., MV 2980; **C**, *Beagiascus pulcherrimus* n. gen., n. sp., CM 35349; **D**, *Kalops diophrys* (Poplin & Lund, 2002) CM 35416 (Poplin & Lund 2002); **E**, *K. monophrys* (Poplin & Lund, 2002), CM 30583 (Poplin & Lund, 2002). Abbreviations: **B**, braincase length; **K**, distance from the posterolateral corner of skull roof to the quadrate condyle; **M**, occlusal edge of maxilla; **P**, posterodorsal edge of preoperculum; **Q**, quadrate; **S**, anterior edge of suboperculum. Anterior to the left, scales bars equal 1 cm, axis scales are identical and arbitrary.

the function of submandibular bones in sarcopterygians as proposed by Pearson (1982). Based on this interpretation, the extralateral gulars found in both species of *Lineagruan* as well as *Beagiascus pulcherrimus* n. gen., n. sp. may have provided greater expansion of the oral-buccal cavities during respiration and feeding. Any relative increase in oral-buccal cavity volume would have led to a greater pressure differential and a stronger suction component to their feeding mechanism.

The geometric consequences of these adaptations suggest differential changes in the volume of the oral-buccal cavity and indicate differences in feeding function. The cheek and cranial differences indicate changes in how the jaws and associated musculature functioned among *L. judithi* n. gen., n. sp., *L. snowyi* n. gen., n. sp., and *B. pulcherrimus* n. gen., n. sp. Increasing the length of the lower jaw creates a jaw optimized for speed while shorter jaws are optimized for more forceful but slower closing during prey capture (Bellwood & Hoey 2004). Given this assessment, the jaws of *L. snowyi* n. sp. and *B. pulcherrimus* n. gen., n. sp. indicate that these fishes may have been better adapted for rapid jaw opening and closing than was *L. judithi* n. gen., n. sp.

It is not known whether the geometric differences in the maxilla-preoperculum-palate-suspensorium complex also result in relative differences in buccal volume, but this possibility cannot be overlooked. The measured and observed differences in the geometry of this complex among species of palaeoniscoids must have a high degree of functional significance to their feeding mechanisms.

Anteopercular bones

The condition of the zone between the opercular apparatus and the cheek region may be important in understanding the type of respiratory mechanism defining these fishes. Among palaeoniscoids, three different morphologies are seen for the zone between the operculum and preoperculum – one

dermohyal plus several anteopercular bones, one or more serial dermohyals, or no intervening bones (Kazantseva-Selezneva 1982). *Lineagruan judithi* n. gen., n. sp., *L. snowyi* n. gen., n. sp., and *Beagiascus pulcherrimus* n. gen., n. sp. are all characterized by the presence of a dermohyal and intervening anteopercular bones.

Kazantseva-Selezneva (1982) proposed that the presence of a series of anteoperculars between the cheek and the operculum could increase the mobility between the palatoquadrate-maxillary complex and the operculum. Kazantseva-Selezneva (1982) proposes two ways by which respiratory intensity could be increased. The first mechanism, when large anteopercular bones are present, would be to decrease the speed at which the operculum moves. The second way an increase in respiratory intensity could be achieved is through a reduction in the size of the anteopercular bones and a concomitant increased lengthening of the operculum (Kazantseva-Selezneva [1982]). Kazantseva-Selezneva (1982) proposed that decreasing the size of the opercular bones would allow for a stronger link between the palatoquadrate-maxillary complex and the operculum as well as a greater amount of water to be ejected.

Following Kazantseva-Selezneva (1982), although *L. judithi* n. gen., n. sp., *L. snowyi* n. gen., n. sp., and *B. pulcherrimus* n. gen., n. sp. all have anteopercular bones, they may have functioned in distinctly different ways. *Lineagruan judithi* n. gen., n. sp. and *L. snowyi* n. gen., n. sp., with their thin, narrow anteopercular bones may fall into the category of decreasing the anteopercular size to allow for an increase in the size of the operculum and a stronger link between this bone and the palatemaxillary complex. *Beagiascus pulcherrimus* n. gen., n. sp. on the other hand, has large, thick, patent anteopercular bones, suggesting that an increase in respiratory intensity may have been obtained by changing the speed in which the operculum is opened and closed.

Operculum

Reconstruction of forces applied to cranial bones by muscles is possible when there are fossilized specimens with preserved muscle attachment sites. The preservation of these attachment sites can be rare. It has been postulated that another feature, the pattern of ganoine ridging, may reflect stress: strain forces similar to those noted for muscle: bone systems (Lund & Younan 1994). Thus, it may prove useful to examine the shape of bones and the pattern of ganoine with the hope of achieving some index of the forces applied to certain bones. The operculum is an exception in that it can show both an attachment site as well as ganoine ridging. In *L. judithi* n. gen., n. sp., a deep concavity is consistently seen in the anterodorsal corner of the operculum. This pit may be a result of an opercular facet located on the underside of the operculum that has been crushed during the preservational process. The opercular facet acts as a hinge point between the operculum and hyomandibular. While this is a typical location for the opercular facet, as seen in extant forms like *Amia*, what is atypical is the corresponding ganoine pattern on the bone (Grande & Bemis 1998).

Typically, the operculum would be strengthened with radiating diagonal ridges similar to *B. pulcherrimus* n. gen., n. sp. and *Amia* (Grande & Bemis 1998). *Lineagruan judithi* n. gen., n. sp. and *L. snowyi* n. gen., n. sp. show continuous vertical ganoine ridges across the opercular-subopercular suture. These continuous ridges may have inhibited or prevented independent movement of these two bones and thus, may have fortified the operculum and suboperculum to work as a single functional unit. This is also supported by fusion of the operculum and suboperculum in *L. judithi* n. gen., n. sp. The postspiracular, with horizontal ridges, is sutured to the dorsal margin of the operculum, close to the opercular facet, in both *L. judithi* n. gen., n. sp. and *L. snowyi* n. gen., n. sp. This strip of bone may have also functioned to strengthen the bone against the forces created by the pulling on the attachment site.

The opercula in *Lineagruan judithi* n. gen., n. sp. and *L. snowyi* n. gen., n. sp. share a common shape and pattern of ganoine. While evidence of the opercular facet is not seen in *L. snowyi* n. gen., n. sp., the similarities in shape and ganoine pattern seen in the opercula of both *L. judithi* n. gen., n. sp. and *L. snowyi* n. gen., n. sp. suggest that these bones

functioned in a similar manner and were subject to similar stresses.

Head and dentition

Sharp recurved or conical teeth are found on the maxilla (including the posteroventral angle) and dentary of *B. pulcherrimus* n. gen., n. sp. *Beagiascus pulcherrimus* n. gen., n. sp. also has a palate that is heavily lined with pointed teeth and tuberculations. *Lineagruan judithi* n. gen., n. sp. is characterized by delicate vertically oriented teeth along the maxilla as well as the dentary. The teeth along the dentary are fine and very difficult to see, as evidenced by their visibility in only one specimen, CM 27401. *Lineagruan snowyi* n. gen., n. sp. has fine, anteriorly inclined teeth on the proportionally shorter maxilla and dentary, suggesting that, like *Cyranorhis bergeraci* and *Wendyichthys dicksoni*, *L. snowyi* n. gen., n. sp. may not have been a macro-predator, but rather fed off of floating particles or small prey items (Lund & Poplin 1997). The geometries of the lateral aspects of the heads of the three species differ strongly, demonstrating that they occupied differing morphospaces, and implying feeding-based fine niche partitioning (for more on fine scale niche partitioning in recent fishes, see Keast & Webb 1966; Gatz 1979).

Phylogenetics

The matrix used in this study was composed of 111 characters and 40 taxa (Appendices 1; 5). It employed taxa for which a majority of the characters were known because highly incomplete taxa of uncertain affinities can produce unstable trees (Wiens 1998; Kearny & Clark 2003; Goloboff *et al.* 2004; Santini & Tyler 2004).

Cladistic analysis of this matrix resulted in two equally parsimonious trees when all characters were run non-additively with the mh* procedure (length 688, ci 38, ri 61). After branch-and-bound treatment to produce the tree with the least amount of homoplasies, one tree resulted with a length of 1272, ci 54, and ri 74 (Fig. 16). The resultant branch-and-bound tree identifies a monophyletic Actinopterygii when sarcopterygian and theoretical outgroups are employed. In general, the topology of this tree reflects the historical appearance as well as the progressive and/or parallel derivation of advanced morphologies.

Within the Actinopterygii, there are three basal groups, one comprised of (*Cheirolepis trailli* (Agassiz, 1835) + the Tarrasiformes [Lund & Poplin, 2002]), the others being the genera *Howqualepis* Long, 1988 and *Mansfieldiscus* Long, 1988. A larger, more derived assemblage comprises the remaining taxa under consideration.

Above this, the Paleoniscimorpha (*sensu* Lund *et al*. 1995) are presented as a polyphyletic grouping, basal to the more derived Holostei, Cladista, and Platysomoids (Fig. 16). The indicated relationships of the latter are such that [Holostei + Cladistia] are the plesiomorphous sister group of the Platysomoids. The Platysomoids and the Cladistia each present distinctively different – but highly specialized, feeding and propulsive adaptations relative to the Holostei and the other fishes analyzed.

Even though this new matrix represents a compilation and revision of previously published matrices (Lund *et al*. 1995; Lund 2000; Lund & Poplin 2002; Cloutier & Arratia 2004), a number of the nodes supported herein were also generated in previous cladistic analyses performed with Bear Gulch fishes and theoretical and/or sarcopterygian outgroups (Lund *et al*. 1995; Lund 2000; Lund & Poplin 2002). These nodes include the Tarrasiformes, Holostei, Cladista, and Platysomoids. This consistency, despite variation in the databases (in terms of included taxa, characters, the identification of character states and their polarities, and the addition of six previously uninvestigated fishes (*Lineagruan judithi* n. gen., n. sp., *L. snowyi* n. gen., n. sp., *Beagiascus pulcherrimus* n. gen., n. sp., Spike [Lund & Grogan pers. comm.], Roundtail [Lund & Grogan pers. comm.], and *Roslerichthys riomafrensis* (Hamel, 2005)) suggests that, given the fossil forms identified to date, these nodes should be considered with some degree of confidence. These nodes are defined by a number of synapomorphic characters and are considered to be robust. For the current analysis it is important to note that the Tarrasiformes (*Paratarrasius* [Lund & Melton, 1982] and *Tarrasius* [Traquair, 1881]) are again proposed to be part of a basal taxon that is separate from the palaeoniscoid fishes (Lund & Poplin 2002). At the other end

of the topology, *Guildayichthys* Lund, 2000 and *Discoserra* Lund, 2000 are also distinctly removed from the larger assemblage as relatively derived Bear Gulch forms, and are presented as the sister taxa to the modern *Polypterus* (Cladistia), as proposed by Lund (2000).

There is also some consistency in the proposed relationships of select palaeoniscoid taxa. In this analysis, the nodes that define (*Kalops monophrys* (Poplin & Lund, 2002) + *K. diophrys* (Poplin & Lund, 2002)), (*Wendyichthys* (Lund & Poplin, 1997) and *Cyranorhis* (Lund & Poplin, 1997)), (*Aesopichthys* (Poplin & Lund, 2000) + *Proceramala* (Poplin & Lund, 2000)), (*Paratarrasisus* (Lund & Melton, 1982) + *Tarrasius* (Traquair, 1881) and (*Palaeoniscum* Blainville, 1818 + *Elonichthys serratus* (Traquair, 1881)) have previously been proposed (Lund & Poplin 2002). This occurred despite modification and expansion of the earlier matrices that were principally based on Bear Gulch fishes. For the present analysis, the RI scores for each character and the characters that define the nodes supporting each sister taxa association are identified in Appendices 2 and 3 respectively.

Relationships of *Beagiascus pulcherrimus* n. gen., n. sp., *Lineagruan judithi* n. gen., n. sp. and *L. snowyi* n. gen., n. sp.

Newly described *Beagiascus pulcherrimus* n. sp., *Lineagruan judithi* n. gen., n. sp., and *L. snowyi* n. gen., n. sp. all fall within the polyphyletic Paleoniscomorpha. Characters and character states defining relevant nodes are identified in Appendix 3. *Lineagruan* represents a terminal clade that is the sister group to *B. pulcherrimus* n. gen., n. sp. and *Roslerichthys. Lineagruan judithi* n. gen., n. sp. and *L. snowyi* n. gen., n. sp. are sister taxa (node 60), collectively defined by features of the anteopercular bones (width and thickness) and by the contact between the nasal and frontal bones. *Lineagruan* differs in the posterior condition of the maxillary, the extent of the anteopercular bones, branchiostegal characteristics, and inclination of the teeth. Additionally, they differ in several morphometric and meristic characters including maximum size (Tables 1; 2; 5; 6; 9; 10). The clade *B. pulcherrimus* n. gen., n. sp. + *Lineagruan* n. gen., is defined by the number and condition of the extrascapular rows, proportions of the posterior plate of the maxilla, and the condition of the branchiostegals below the mandible. *Beagiascus pulcherrimus* n. gen., n. sp. is distinguished by numerous cranial and postcranial characters (Appendix 3). The association between *Roslerichthys* (based upon one specimen), *B. pulcherrimus* n. gen., n. sp., and *Lineagruan*, is weakly supported. This tree proposes that *Lineagruan judithi* n. gen., n. sp. and *L. snowyi* n. gen., n. sp. are more closely related to each other than either is to *Beagiascus pulcherrimus* n. gen., n. sp. or any of the other fishes investigated in this study. This pattern of relatedness is consistent with the analyses based upon meristic and morphometric data.

Geometry of cranial bones

As evidenced by Figure 15, suites of differences in the lengths and inclinations of cranial and suspensorial bones characterize the species of palaeoniscoids that have been quantitatively analyzed (Lund & Poplin 1997, 1999; Poplin & Lund 2002). This same set of observations has also been noted for *L. judithi* n. gen., n. sp., *L. snowyi* n. gen., n. sp., and *B. pulcherrimus* n. gen., n. sp. (Table 13). These suites of mutually variable cranial characteristics also distinctly separate the three species of fishes in discriminant and principle components analyses, and so, are considered to be more significant than any subjectively interpreted individual character from these morphological complexes. It is particularly noteworthy that in the case of the three species investigated above, many of the highly ranked measurements in the Principle Components Analysis are not characters normally used in either diagnoses or cladistic analyses (Table 13). The ecomorphological significance of this variation warrants further investigation.

CONCLUSIONS

Meristic, morphometric, and cladistic analyses represent independent analytical approaches to assess morphological data. All approaches support the distinct separation of *Lineagruan judithi* n. gen., n. sp., *L. snowyi* n. gen., n. sp., and *Beagiascus*

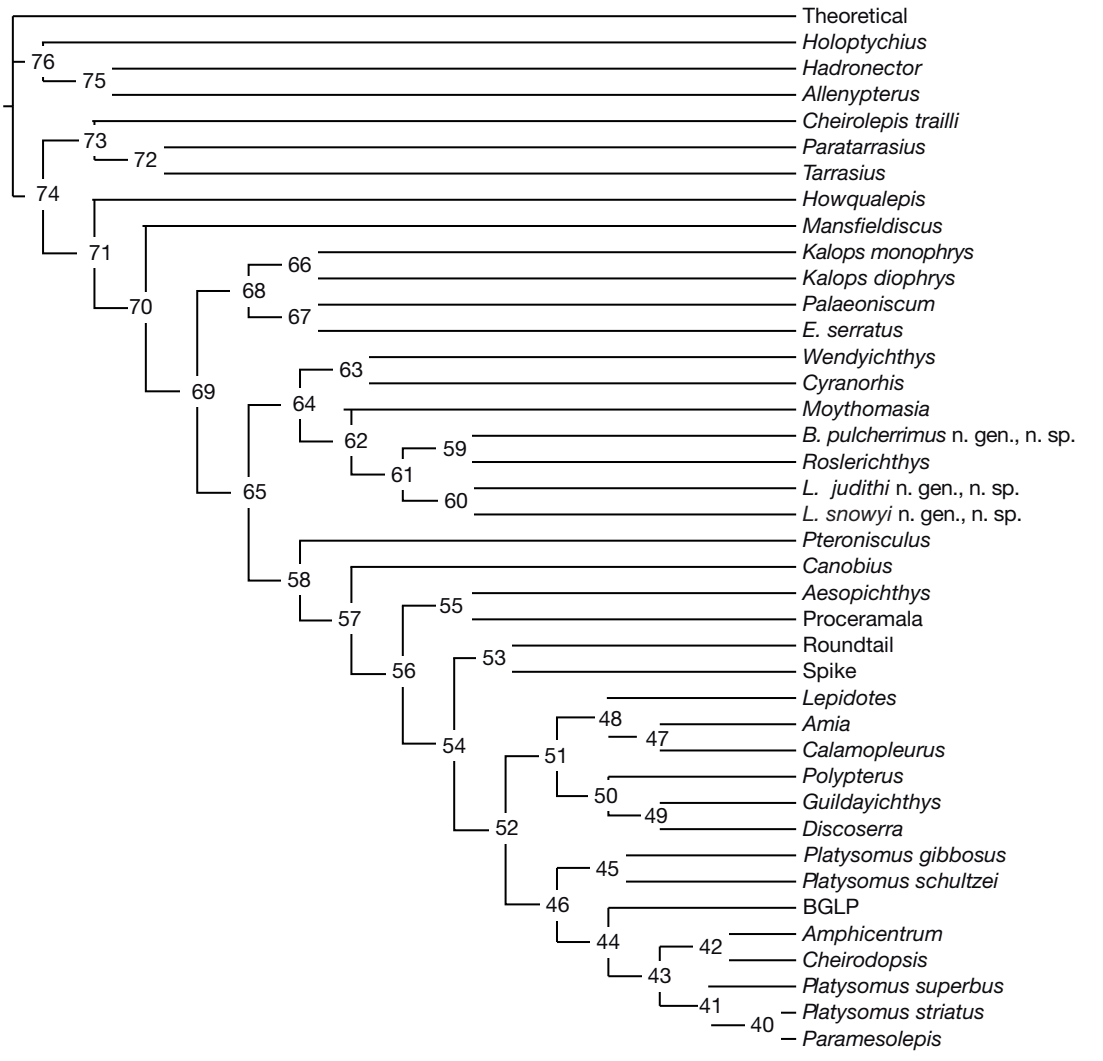

FIG. 16. — Proposed relationships of actinopterygians. Characters were treated non-additively, resulting in two trees with length of 688, ci of 38, and ri of 61. Branch-and-bound treatment resulted in one tree, presented above with a length of 1272, ci of 54 and ri of 74. See Appendix 1 for characters and character states, Appendix 2 for RI scores for each character, and Appendix 3 for characters supporting each node. Abbreviations: ***B.***, *Beagiascus*; ***E.***, *Elonichthys*; ***L.***, *Lineagruan*.

pulcherrimus n. gen., n. sp. – but advocate a closer relationship between the *Lineagruan* n. gen. species. *Lineagruan judithi* n. sp. cannot be considered a younger version of *L. snowyi* n. gen., n. sp. by virtue of the well-ossified neurocrania alone. The morphospace defined for each of the *Lineagruan* species and *B. pulcherrimus* n. gen., n. sp. and the meristic and morphometric analyses corroborate the separation of these taxa into two genera, as well as the sister taxon status of *Lineagruan judithi* n. gen., n. sp. and *L. snowyi* n. gen., n. sp. This is also supported by the cladistic analysis.

Anatomical, morphometric, and cladistic analyses of *Lineagruan judithi* n. gen., n. sp. and *L. snowyi* n. gen., n. sp. suggest that differences between these forms involve variations within character complexes

TABLE 13. — Rotated component matrix of natural logarithms of cheek measurements (angular measures omitted). Two components were extracted via Principle Component Analysis; varimax rotation with Kaiser normalization. Rotation converged in three iterations. Abbreviations: see Table 3.

	Component 1	Component 2
IOQ	0.941	0.095
SQ	0.93	0.229
ML	0.914	0.252
BCL	0.914	0.314
OH	0.912	0.002
SIO	0.912	0.298
MH	0.891	0.13
SH	0.866	0.374
MPL	0.865	0.13
SKQ	0.822	0.134
SIO2	0.718	0.014
PH	0.46	0.651
OW	0.053	-0.919

that may have been influential in propulsive as well as feeding and/or respiratory specializations. These differences in functional regimes may have allowed for fine-scale niche partitioning within the Bear Gulch bay. This said, the polyphyly of the Paleoniscimorpha presented in this branch-and-bound tree simply reflects the information included in this database of characters, the character states used, and on the taxa analyzed. However, approximately 70% of putative Bear Gulch actinopterygian taxa recovered remain to be analyzed. Thus, this analysis of early actinopterygians represents a work in progress.

Acknowledgements
We thank G. Arratia and R. Cloutier for sharing their cladistic database with us, and for their stimulating discussions.

We thank the Montana ranch families for their long history of generosity. This research would not have been possible without the Bear Gulch Field Crew and countless volunteers. Field work and research in the Bear Gulch have been supported by the Bear Gulch Research Fund, the Center for Field Research, NSF grants BMS 75-02720, DEB 75-02720, DEB 77-02548, DEB 79-19492, as well as grants from the Carnegie Museum of Natural History, Royal Ontario Museum, St. Joseph's University, and the Bryn Mawr Paleontological Fund.

This research was originally performed by Kathryn Mickle as a Masters thesis at St. Joseph's Universityor a NSF GK-12 Fellowship (NSF GK-12 0139303) in association with the Wagner Free Institute of Science. Queries regarding the data matrix should be addressed to Richard Lund. Not including the new species presented in this paper, the taxa coding for phylogenetic analyses was performed by R. Lund. We thank the members of K. Mickle's M. S. Thesis committee, J. Thompson and S. McRobert, for their advice. We thank F. Abe and M. Davis for use of camera equipment.

This manuscript has been greatly improved through the comments from an anonymous reviewer of an earlier version of this work and the two reviewers of this version. Many thanks go to the reviewers for the time they have put into this paper.

REFERENCES

AGASSIZ L. 1835. — *Recherches sur les poissons fossiles*, vol. 2. Imprimerie de Petitpierre et Prince, Neuchâtel, 310 p.

ALDINGER H. 1937. — Permisches Ganoidfishe aus Ostgrønland. *Meddelelser om Grønland* 102: 1-392.

ALLIS E. P. 1922. — The cranial anatomy of *Polypterus*, with special reference to *Polypterus bichir. Journal of Anatomy* 56: 189-294.

ARRATIA G. 2008. — Actinopterygian postcranial skeleton with special reference to the diversity of fin ray elements, and the problems of identifying homologies, *in* ARRATIA G., SCHULTZE H.-P. & WILSON M. V. H. (eds), *Mesozoic Fishes 4 – Homology and Phylogeny.* Verlag Dr Friedrich Pfeil, München: 49-101.

BELLWOOD D. & HOEY A. 2004. — Feeding in Mesozoic fishes: a functional perspective, *in* ARRATIA G. & TINTORI A. (eds), *Mesozoic Fishes 3 – Systematics, Paleoenvironments and Biodiversity.* Verlag Dr Friedrich Pfeil, München: 639-649.

CAMPBELL K. S. W. & PHUOC L. D. 1983. — A Late Permian Actinopterygian fish from Australia. *Journal of Palaeontology* 26: 33-70.

COATES M. I. 1993. — New Actinopterygian fish from the Namurian Manse Burn Formation of Bearsden, Scotland. *Palaeontology* 36: 123-146.

CLOUTIER R. & ARRATIA G. 2004 — Early diversification of Actinopterygians, *in* ARRATIA G., WILSON M. V. H. & CLOUTIER R. (eds), *Recent Advances in the Origin and Early Radiation of Vertebrates*. Verlag Dr Friedrich Pfeil, München: 217-270.

DI CANZIO J. A. 1985. — Ecomorphology of the Os-

teichthyes from the Bear Gulch Limestone, *in* DUTRO T. & PFEFFERKORN H. W. (eds), *Compte Rendu, neuvième Congrès international de Stratigraphie et de Géologie du Carbonifère* 5: 501-512.

DYNE M. B. 1939. — The skull of *Amphicentrum granulosum. Proceedings of the Zoological Society of London*, Series B, 109: 195-210.

FARRIS J. S. 1986. — *Hennig86. Version 1.5*. Software program and documentation. Published by the author, Port Jefferson Station, New York.

FERRY L. A. & LAUDER G. V. 1996. — Heterocercal tail function in leopard sharks: a three-dimensional kinematic analysis of two models. *Journal of Experimental Biology* 199: 2253-2268.

GARDINER B. G. 1984. — *Devonian Paleoniscid Fishes – New Specimens of* Mimia *and* Moythomasia *from the Upper Devonian of Western Australia.* University of California Press, Berkeley, California, 428 p.

GATZ A. J. JR 1979. — Community organization in fishes as indicated by morphological features. *Ecology* 60: 711-718.

GOLOBOFF P. A., FARRIS J. S. & NIXON K. 2004. — *T.N.T. Tree Analysis Using New Technology*. Version 1.0.

GRANDE L. & BEMIS W. E. 1998. — A comprehensive phylogenetic study of amiid fishes (Amiidae) based on comparative skeletal anatomy. An empirical search for interconnected patterns of natural history. *Society of Vertebrate Paleontology*, Supplement 1, *Memoir* 4: 1-690.

GROGAN E. D. & LUND R. 2002. — The geological and biological environment of the Bear Gulch Limestone (Mississippian of Montana, USA) and a model for its Deposition. *Geodiversitas* 24 (2): 295-315.

HAMEL M. H. 2005. — A new lower Actinopterygian from the Early Permian of the Paraná Basin, Brazil. *Journal of Vertebrate Paleontology* 25:19-26.

HARRIS R. J. 1975. — *A Primer of Multivariate Statistics*. Academic Press Inc., New York, 322 p.

HELFMAN G. S., COLLETTE B. B. & FACEY D. E. 1997. — *The Diversity of Fishes*. Blackwell Science, Malden, USA, 528 p.

JANVIER P. 2002. — *Early Vertebrates*. Oxford University Press, Oxford, England, 393 p.

JARVIK E. 1948. — On the morphology and taxonomy of the Middle Devonian Osteolepid fishes of Scotland. *Kungl Svenska Vetenskapsakademiens Handlingar* (3) 25: 1-301.

KAZANTSEVA-SELEZNEVA A. A. 1982. — The Phylogeny of the Lower Actinopterygians. *Journal of Ichthyology* 21: 579-594. English translation 1982, 21: 1-16 Scripta Publishing, Silver Spring, Maryland.

KEARNY M. & CLARK J. M. 2003. — Problems due to Missing Data in Phylogenetic Analyses Including Fossils: A Critical Review. *Journal of Vertebrate Paleontology* 23 (2): 263-274.

KEAST J. A. & WEBB D. 1966. — Mouth and body form relative to feeding ecology in the fish fauna of a small lake, Lake Opinicon, Ontario. *Journal of the Fisheries Research Board of Canada* 23: 1835-1874.

LIAO J. & LAUDER G. V. 2000. — Function of the heterocercal tail in white sturgeon: flow visualization during steady swimming and vertical maneuvering. *Journal of Experimental Biology* 203: 3585-3594.

LIEM K. F., BEMIS W. E., WARREN F. W. JR & GRANDE L. 2001. — *Functional Anatomy of the Vertebrates – an Evolutionary Perspective*. Harcourt College Publishers, Fort Worth, USA, 703 p.

LONG J. A. 1988. — New palaeoniscoid fishes from the Late Devonian and Early Carboniferous of Victoria. *Association of Australasian Paleontologists Memoir* 7: 1-64.

LOWNEY K. A. 1980. — *Certain Bear Gulch (Namurian A, Montana) Actinopterygii (Osteichthyes) and a Reevaluation of the Evolution of the Paleozoic Actinopterygians*. Unpublished Ph.D. Thesis, New York University, USA, 489 p.

LUND R. 2000. — The new Actinopterygian order Guildayichthyiformes from the Lower Carboniferous of Montana (USA). *Geodiversitas* 22 (2):171-206.

LUND R. & LUND W. L. 1985. — The coelacanths from the Bear Gulch Limestone (Namurian) of Montana and the evolution of the coelacanthiformes. *Bulletin of the Carnegie Museum of Natural History* 25: 1-74.

LUND R. & MELTON W. G. JR 1982. — New Actinopterygian fish from the Mississippian Bear Gulch Limestone of Montana. *Palaeontology* 25: 485-498.

LUND R. & POPLIN C. 1997. — The Rhadinichthyids (Palaeoniscoid Actinopterygians) from the Bear Gulch Limestone of Montana (USA, Lower Carboniferous). *Journal of Vertebrate Paleontology* 17: 466-486.

LUND R. & POPLIN C. 1999. — Fish diversity of the Bear Gulch Limestone, Namurian, Lower Carboniferous of Montana, USA. *Geobios* 32: 285-295.

LUND R. & POPLIN C. 2002. — Cladistic analysis of the relationships of the tarrasiids (Lower Carboniferous Actinopterygians). *Journal of Vertebrate Paleontology* 22: 480-486.

LUND R., POPLIN C. & MCCARTHY K. 1995. — Preliminary analysis of the interrelationships of some Paleozoic Actinopterygii. *Geobios* Mem. Spec. 19: 215-220.

LUND R. & YOUNAN I. 1994. — The functional significance of Paleozoic Actinopterygian skull bone ganoine patterns (abstract), *American Society of Ichthyologists and Herpetologists 74th Annual Meeting; 1994 June 2-8.* Los Angeles: American Society of Ichthyologists and Herpetologists: 163.

MOY-THOMAS J. A. & DYNE M. B. 1938 — Actinopterygian fishes from the Lower Carboniferous of Glencartholm, Eskdale, Dumfriesshire. *Transactions of the Royal Society of Edinburgh* 59: 437-480.

MOY-THOMAS J. A. & MILES R. S. 1971. — *Palaeozoic Fishes*. W. B. Saunders Company, Philadelphia, 257 p.

NIELSEN E. 1942. — Studies on Triassic fishes from East Greenland. 2. *Glaucolepis* and *Boreosomus. Palaeozoologica Groenlandica* 1: 1-403.

NIXON K. C. 2002. — *Winclada (BETA) ver. 1.00.08*. Published by the author, Ithaca, New York.

PEARSON D. M. 1982. — Primitive bony fishes, with special reference to *Cheirolepis* and palaeonisciform Actinopterygians. *Zoological Journal of the Linnean Society*, London, 74: 35-67.

PEHRSON T. 1947. — Some new interpretations of the skull in *Polypterus*. *Acta Zoologica* 28: 400-455.

PEHRSON T. 1958. — The early ontogeny of the sensory lines and the dermal skull in *Polypterus. Acta Zoologica* 39: 241-258.

POPLIN C. 2004. —The dermosphenotic in early Actinopterygians, a nomenclatural problem, *in* ARRATIA G. & TINTORI A. (eds), *Mesozoic Fishes 3 – Systematics, Paleoenvironments and Biodiversity.* Verlag Dr Friedrich Pfeil, München: 165-178.

POPLIN C. & LUND R. 2000. — Two new deep-bodied Actinopterygians from Bear Gulch, (Montana, USA, Lower Carboniferous). *Journal of Vertebrate Paleontology* 20: 428-449.

POPLIN C. & LUND R. 2002. — Two Carboniferous fine-eyed palaeoniscoids (Pisces, Actinopterygii) from Bear Gulch (USA). *Journal of Paleontology* 76: 1014-1028.

SANTINI F. & TYLER J. C. 2004. — The importance of even highly incomplete fossil taxa in reconstructing the phylogenetic relationships of the Tetraodontiformes (Acanthomorpha: Pisces). *Integrative and Comparative Biology* 44: 349-357.

SCHAEFFER B. & ROSEN D. E. 1961. — Major adaptive levels in the evolution of the Actinopterygian feeding mechanism. *American Zoologist* 1: 187-204.

SCHULTZE H.-P. & ARRATIA G. 1989. — The composition of the caudal skeleton of teleosts (Actinopterygii: Osteichthyes). *Zoological Journal of the Linnean Society* 97: 189-231.

TAVERNE L. 1996. — Ostéologie et position systématique des Tarrassiiformes, Actinoptérygiens (Pisces) du Carbonifère de l'Écosse et des États-Unis. *Biologisch Jaarboek Dodonaea* 64: 138-159.

TINTORI A. 1996. — *Paralepidotus ornatus* (Agassiz 1833-43): a semionotid from the Norian (Late Triassic) of Europe, *in* ARRATIA G. & VIOHL G. (eds), *Mesozoic Fishes – Systematics and Paleoecology*. Verlag Dr Friedrich Pfeil, München: 167-179.

TRAQUAIR R. H. 1879. — On the structure and affinities of the Platysomidae. *Transactions of the Royal Society of Edinburgh* 29: 343-391.

TRAQUAIR R. H. 1881. — Report on fossil fishes collected by the Geological Survey of Scotland in Eskdale and Liddlesdale. Part 1, Ganoidei. *Transactions of the Royal Society of Edinburgh* 30: 15-71.

VIDELER J. J. 1996. — *Fish Swimming*. Chapman and Hall, London, 260 p.

WIENS J. J. 1998. — Does adding characters with missing data increase or decrease phylogenetic accuracy? *Systematic Biology* 47 (4): 625-640.

WILGA C. D. & LAUDER G. V. 2002. — Function of the heterocercal tail in sharks: quantitative wake dynamics during steady horizontal swimming and vertical maneuvering. *Journal of Experimental Biology* 205: 2365-2374.

WILLIAMS L. A. 1983. — Deposition of the Bear Gulch Limestone: a Carboniferous Plattenkalk from Central Montana. *Sedimentology* 30: 843-860.

WOODWARD A. S. 1895. — *Catalogue of the Fossil Fishes in the British Museum (Natural History).* Part 2. British Museum (Natural History), London, 544 p.

ZHU MIN & SCHULTZE H. P. 2001. — Interrelationships of basal osteichthyans, *in* ZHU AHLBERG P. E. (ed.), *Major Events in Early Vertebrate Evolution*. Taylor & Francis, London: 289-314.

ZIDEK J. 1992. — Late Pennsylvanian Chondrichthyes, Acanthodii, and deep-bodied Actinopterygii from the Kinney Quarry, Manzanita Mountains, New Mexico. *New Mexico Bureau of Mines and Mineral Resources Bulletin* 138: 145-182.

Submitted on 16 January 2008;
accepted on 26 January 2009.

APPENDIX 1

Characters and character states for the cladistic analysis. Abbreviations: **Ao**, antorbital; **BR**, branchiostegal ray; **BR2**, second branchiostegal ray; **b/t**, between; **dpt**, dermopterotic; **dsp**, dermosphenotic; **ht/l**, height/lenght; **Io**, infraorbital; **op**, operculum; **pop**, preoperculum; **Pdio**, posterodorsal infraorbital; **Pvio**, posteroventral infraorbital; **Rpr**, rostropostrostral; **So**, suborbital; **sop**, suboperculum.

Character	State 0	State 1	State 2	State 3	State 4	State 5
0 mouth	subterminal	terminal				
1 snout shape	blunt rounded	sharp bump	upswept (upturned)	notch	sharp	beak
2 premaxillary position	sutured broadly in midline	sutured narrowly in midline	do not meet in midline, sutured laterally to antorbital	lateral and loose, unsutured	median, loose	absent as distinct bone
3 premaxillary condition	sutured to rostral bones	loose, unsutured	fused to antorbital	sutured to frontals (nasal process)	absent	
4 rostral fusion	separate bone or bones (no fusion)	fused to postrostral	fused to premaxilla	fused to premaxilla and postrostral	absent	
5 rostral numbers	many	paired	single median	reduced to many	absent as distinct bone	
6 rostral position	excluded from oral margin	in notch in oral margin	b/t premaxilla, in oral margin	absent		
7 rostral notch shape	absent	vertical	keyhole-shape			
8 ethmoid commissure	across midline	not across midline	absent			
9 postrostrals	mosaic	several median	single median	paired	median and paired	absent
10 Io canal, ethmoid commissure, and So canal intersect	in sutures	meet in single bone (antorbital)	So canal does not connect			
11 antorbital presence	absent as distinct bone	distinct, separate	fused to premaxilla			
12 antorbital shape	absent as distinct bone	rhombic	inverted L	vertical pillar	recumbent	extremely long
13 antorbital location	absent	posterolateral to rostral Rpr	terminal in midline			
14 nasals	numerous, serial	2 per side	1 per side	absent		
15 narial notches	nasals not notched for nares	anterior narial notch only	anterior and posterior narial notches	absent		
16 nasal posterior contact	frontal	dermosphenotic	posterodorsal infraorbital			
17 supraorbitals	double series	single series	single bone	absent		
18 tectals	present	absent				
19 frontals	many	1 pair	2 pairs			
20 parietal/frontal ratio	subequal	much smaller parietal	much larger parietal			
21 pineal opening	in postrostral area	in frontal (parietal) area	absent			
22 supraorbital canal course	through/under supraorbital bones	under frontal/ supraorbital suture	through/under frontals, supraorbitals lack canal	through/under frontals, supraorbitals absent		
23 supraorbital canal trajectory	into parietal (postparietal)	into frontal (parietal)	into dpt (intertemporal)			
24 lateral otic margin	parallel to midsagittal line	approaches midline posteriad	diverges from midline posteriad			
25 otic canal bones	3 bones	dsp and dpt (2 bones)	dermopterotic only (1 bone)	fused to parietal		
26 otic-preopercular canal contact	absent	present				
27 infraorbital canal	to dermosphenotic	to dermopterotic	to fused dpt-parietal	to frontal		
28 intracranial joint 1	otoccipital/ethmosphenoid dorsal	absent				

Character	State 0	State 1	State 2	State 3	State 4	State 5
29 intracranial joint 2	ventral articulation b/t otoccipital/ethmosphenoid	absent				
30 supraoccipital	absent	only on braincase	on skull roof			
31 supratemporal commissure	across midline	not across midline	loop to skull roof			
32 extrascapulars, principle row	3 bones	1 pair	2 pairs	5 or more	canal bones only	
33 extrascapular rows	1 row	2 separate rows	2 rows, shared median bone	absent		
34 posteroventral lo is	second	first	third	> third		
35 posterodorsal lo is	third	fourth	fifth	sixth	> sixth	second
36 posterodorsal lo shape	narrow rectangular	T-shaped	reverse L-shaped	expanded		
37 suborbital numbers	none	2-5 large, 1 row	more than 1 row	large one with canal	mosaic	1 small
38 suborbital fit	absent	sutured/overlap	loose, gaps			
39 suborbital thickness	absent	thick	thin, no ganoine			
40 suborbital insertion b/t max & Pvio	suborbitals absent	none	suborbital inserted	no contact		
41 maxilla posterior end	posterior to orbit	orbital	preorbital	absent		
42 maxilla posterior plate	not differentiated from anterior part	moderate rectangular plate	high rounded	high triangle	absent	
43 maxilla postero-ventral process	absent	slightly developed process	strong process			
44 maxilla mobility	absent, fused to cheek	free from cheek	maxilla absent			
45 marginal teeth in upper jaw midline	present	absent				
46 anterior end of maxilla	preorbital	orbital	postorbital	maxilla absent		
47 posterior maxillary proportions (ht/l)	< 0.3	0.35-0.99	1.0-1.3	> 1.3	absent	
48 maxillary teeth	marginal, acrodont	pleurodont	mesial surface of maxilla	absent		
49 supramaxilla	absent	present				
50 mandible dentary proportion	less than 40%	greater than 60%				
51 mandible coronoid process	absent	present				
52 marginal tooth orientation	vertical	forwardly inclined	posteriorly inclined	pleurodont	absent	
53 marginal tooth extent	length of jaws	anterior half only	restricted to front	absent		
54 dentition type	marginal	coronoid-palatal	phyllodont			
55 preopercular bone numbers	2 subequal bones	1 bone	big dorsal-small ventral bone			
56 dorsal preopercular/ squamosal shape	squamosal polygonal plate(s)	hatchet-shaped	diamond-shaped	tall, narrow		
57 preopercular canal dorsally	to mid-otic region	to postorbital corner	to posterior otic region	ends blindly in squamosal		
58 preopercular canal ventrally	to mandible	ends blindly in preoperculum	absent			
59 preoperculum, anterior contact	pop absent	suborbitals	infraorbitals, extensive	no anterior contact	fused to sub-orbitals	
60 preopercular angle	pop absent	> 50°	35-50°	25-34°	15-24°	
61 jugal (horizontal) line	complete canal	long pit line of preopercular	short pit line on preopercular	absent		
62 dermohyal	absent	one	two	vertical series		

Character	State 0	State 1	State 2	State 3	State 4	State 5
63 anteopercular numbers	absent	few (1-5)	single series	variable		
64 anteoperculars	absent	not to bottom of opercular	to bottom of opercular	to bottom of subopercular		
65 anteopercular width	absent	uniform width	widens ventrally	tapers ventrally		
66 anteopercular thickness	absent	same as adjacent bones	extremely thin			
67 subopercular upper suture	horizontal	diagonal	concave	sigmoidal	convex	absent
68 subopercular lower suture	horizontal	diagonal	concave	sigmoidal	convex	absent
69 subopercular height	< opercular	= opercular	> opercular	<< opercular	absent	
70 op sop anterior margin alignment	< 16° difference	17-26° difference	40-46° difference	> 46° difference	absent	
71 interoperculum	absent	present				
72 first branchio stegal height	not distinctly different than second, thin	twice the height of BR2, strap-like	> twice height of BR2	absent		
73 branchiostegals below mandible	9-12	7-8	3-6	0-1		
74 branchiostegals behind mandible	smooth transition	distinct shortening	triangular plate	absent		
75 extralateral gular	absent	present				
76 gular, median	shorter than lateral gular	longer than lateral gular	absent			
77 gular, lateral	broader than next BR	like next BR	much extended	absent		
78 submandibulars	present	absent				
79 clavicle length	short	elongate	absent			
80 interclavicle	absent	present				
81 postspiraculars	absent	several, unsutured	single unsutured	single, sutured to opercular		
82 presupracleithrum	present	absent				
83 sclerotics	many	3 or 4	2	absent		
84 parasphenoid	short	length of braincase				
85 suspensorium	met-autostyly	limited methyostyly	extensive methyostyly			
86 dorsal fin number	2	1				
87 first dorsal position	forward	posterior	absent			
88 2nd dorsal/anal fin origin position	dorsal anterior to anal	dorsal above anal	dorsal behind anal			
89 2nd dorsal/anal fin rays	tightly packed	rear rays spaced apart	all rays spaced apart	anterior rays immobile/unjointed		
90 2nd dorsal fin length	short	rear close to caudal	merged with caudal			
91 2nd dorsal fin shape	triangular	sigmoidal	elongate			
92 dorsal fin specializations	none, triangular	elongate, low	long acuminate	long and high	polypterid	
93 2nd dorsal fin base	no specializations	scaled lobe	guard scales	basal plate and axis		
94 pectoral fin base	endoskeletal axis, unibasal	serial radials				
95 pectoral scaled lobe	present	absent				
96 pelvic fin	normal proportions (triangular)	elongate (long-based)	reduced or absent			
97 caudal axis	heterocercal	hemiheterocercal	diphycercal			
98 caudal outline	cleft equilobate	strongly inequilobate	rounded	pointed		
99 predorsal ridge scales	absent	few (3-5)	many	complete to occiput		
100 precaudal dorsal ridge scales	absent	few (3-5)	continuous b/t fins			

Character	State 0	State 1	State 2	State 3	State 4	State 5
101 precaudal ventral ridge scales	absent	few (3-5)	continuous b/t fins			
102 anal fin base	basal plate	serial infrahemal-radial				
103 anal fin base length	short	anal end close to caudal	merged with caudal			
104 caudal fin rays	not webbed	webbed				
105 scale type	rhombic ganoid	with pore system	cosmoid	cycloid		
106 scale row inversion	progressive	abrupt	absent			
107 flank scales	same proportions as others	very tall	tall, cristate	micromeric		
108 ventrolateral flank scales	same proportions as others	very narrow	micromeric			
109 body form, lateral view	fusiform/elongate	ovoid	high dorsum, flatter venter	round	angulated	
110 highest/lowest points of body profile	no specializations	ridge scutes	few specialized scales	ridge scale/dorsal fin scales		

APPENDIX 2

RI scores for each character. See Appendix 1 for characters description.

Character	RI	Character	RI	Character	RI	Character	RI
0	68	28	100	56	84	84	100
1	70	29	100	57	57	85	88
2	60	30	100	58	0	86	100
3	71	31	53	59	78	87	100
4	63	32	31	60	68	88	0
5	57	33	66	61	66	89	64
6	33	34	37	62	68	90	87
7	0	35	36	63	100	91	64
8	33	36	69	64	100	92	30
9	71	37	75	65	100	93	70
10	75	38	68	66	80	94	80
11	66	39	71	67	20	95	64
12	81	40	69	68	28	96	33
13	80	41	33	69	54	97	62
14	70	42	71	70	63	98	40
15	46	43	73	71	75	99	63
16	70	44	100	72	25	100	62
17	41	45	58	73	61	101	53
18	100	46	20	74	55	102	75
19	83	47	70	75	75	103	64
20	50	48	44	76	50	104	66
21	0	49	100	77	50	105	80
22	66	50	50	78	0	106	43
23	33	51	72	79	81	107	100
24	46	52	66	80	0	108	87
25	53	53	60	81	100	109	57
26	20	54	63	82	66	110	42
27	38	55	57	83	42		

APPENDIX 3

Characters and character states at nodes for Figure 16. See Appendix 1 for abbreviations.

Node	Character		State	
76				
	0	mouth	1	terminal
	24	lateral otic margin	2	diverges from midline posteriad
	73	branchiostegals below mandible	3	0 or 1
	93	second dorsal fin base	3	basal plate and axis
	105	scale type	1	with pore system
	106	scale row inversion	1	abrupt
	109	body form, lateral view	1	ovoid
75				
	2	premaxillary position	2	do not meet in midline, sutured laterally to So
	23	supraorbital canal, trajectory of	2	into Dpt (intertemporal)
	34	posteroventral lo is	1	first
	35	posterodorsal lo is	5	second
	41	maxilla posterior end	3	absent
	42	maxilla posterior plate	5	absent as distinct bone
	45	marginal teeth in upper jaw midline	1	absent
	46	anterior end of maxilla	3	maxilla absent
	47	posterior maxillary proportions	4	absent
	48	maxillary teeth	3	absent
	51	mandible coronoid process	1	present
	67	subopercular upper suture	1	diagonal
	72	first branchiostegal height	3	absent
	74	branchiostegals behind mandible	1	distinct shortening
	77	gular, lateral	3	absent
	89	second dorsal/anal fin rays	2	all rays spaced apart
	97	caudal axis	2	diphycercal
	104	caudal fin rays	1	webbed
74				
	9	postrostrals	1	several median
	10	lo canal, ethmoid comm, So canal	1	meet in single bone (antorbital)
	15	narial notches	2	anterior and posterior narial notches
	19	frontals	1	1 pair
	28	intracranial joint 1	1	absent
	29	intracranial joint 2	1	absent
	36	posterodorsal io shape	1	t-shaped
	42	maxilla posterior plate	1	moderate rectangular plate
	55	preopercular bone numbers	1	1 bone
	56	dorsal preopercular/squamosal shape	1	hatchet-shaped
	59	preoperculum, anterior contact	1	suborbitals
	60	preopercular angle	4	15-24°
	62	dermohyal	1	1
	85	suspensorium	2	extensive methyostyly
	86	dorsal fin number	1	1
	87	first dorsal position	2	absent
	94	pectoral fin base	1	serial radials
	102	anal fin base	1	serial infrahemal-radial
73				
	107	flank scales	3	micromeric
	108	ventrolateral flank scales	2	micromeric
72				
	11	antorbital presence	1	distinct, separate
	12	antorbital shape	1	rhombic
	13	antorbital location	1	posterolatral to rostral/Rpr
	14	nasals	1	2 per side
	19	frontals	2	2 pairs
	89	second dorsal/anal fin rays	2	all rays spaced apart
	90	second dorsal fin length	2	merged with caudal
	91	second dorsal fin shape	2	elongate
	96	pelvic fin	2	reduced/absent

Node	Character		State	
	97	caudal axis	2	diphycercal
	98	caudal outline	3	pointed
	103	anal fin base	2	merged with caudal
71				
	14	nasals	2	1 per side
	17	supraorbitals	3	absent
	18	tectals	1	absent
	20	parietal/frontal ratio	1	much smaller parietal
	99	predorsal ridge scales	1	few (3-5)
	101	precaudal ventral ridge scales	1	few (3-5)
70				
	11	antorbital presence	1	distinct, separate
	12	antorbital shape	1	rhombic
	13	antorbital location	1	posterolateral to rostral/Rpr
	37	suborbital numbers	1	2-5 large, 1 row
	39	suborbital thickness	1	thick
69 Paleoniscomorpha				
	9	postrostrals	2	several median
	106	scale row inversion	1	abrupt
68				
	17	supraorbitals	1	single series
	22	supraorbital canal course	2	through/under frontals, supraorbitals lack canal
	35	posterodorsal lo is	2	fifth
	36	posterodorsal lo shape	0	narrow rectangular
67				
	69	subopercular height	1	equal to opercular
66				
	76	gular, median	1	longer than lateral gular
	89	second dorsal/anal fin rays	1	rear rays spaced apart
	91	second dorsal fin shape	1	sigmoidal
	95	pectoral scaled lobe	0	present
65				
	4	rostral fusion	1	fused to postrostral
	5	rostral numbers	4	absent as distinct bone
	16	nasal posterior contact	2	Pdio
64				
	93	second dorsal fin base	2	guard scales
	108	ventrolateral flank scales	1	very narrow
63				
	2	premaxillary position	5	absent as a distinct bone
	3	premaxillary condition	4	absent
	6	rostral position	1	in notch in oral margin
	45	marginal teeth in upper jaw midline	1	absent
	52	marginal tooth orientation	1	forwardly inclined
	76	median gular	1	longer than lateral
62				
	63	anteopercular numbers	2	single series
	64	anteoperculars	2	to bottom of opercular
	65	anteopercular width	2	widens ventrally
	66	anteopercular thickness	1	same as adjacent bones
61				
	33	extrascapular rows	2	2 rows, shared median
	47	posterior maxillary proportions	0	< 0.3
	74	branchiostegal rays behind mandible	1	distinct shortening
60				
	16	nasal posterior contact	0	with frontal
	65	anteopercular bone width	1	uniform width
	66	anteopercular thickness	2	thin
***Lineagruan judithi* n. gen., n. sp.**				
	42	maxilla posterior plate	2	high rounded
	73	branchiostegals below mandible	2	3-6
***Lineagruan snowyi* n. gen., n. sp.**				
	27	infraorbital canal	1	to dermopterotic
	52	marginal tooth orientation	1	fowardly inclined

Node	Character		State	
	64	anteoperculars	3	extends to bottom of suboperculum
	72	first branchiostegal height	1	twice the height of BR2
59				
	93	second dorsal fin base	0	no specializations
***Beagiascus pulcherrimus* n. gen., n. sp.**				
	2	premaxillary position	1	sutured narrowly in midline
	27	infraorbital canal	1	to dermopterotic
	68	subopercular lower suture	2	concave
	72	first branchiostegal height	1	twice the height of BR2
	88	second dorsal fin/anal fin position	1	dorsal above anal
	100	precaudal dorsal ridge scales	2	continuous between fins
58				
	0	mouth	1	terminal
	36	posterodorsal lo shape	1	T-shaped
57				
	40	suborbital insertion	1	no suborbital inserted b/t maxilla and Pvio
	42	maxilla posterior plate	2	high rounded
	56	dorsal preopercular/squamosal shape	2	diamond shape
	60	preopercular angle	1	> 50°
	70	opercular subopercular anterior margin	0	< 16° difference
	99	predorsal ridge scales	2	many
	103	anal fin base length	1	anal end close to caudal
56				
	3	premaxillary condition	1	loose, unsutured
	51	mandible coronoid process	1	present
	90	second dorsal fin length	1	rear close to caudal
55				
	89	second dorsal and anal fin rays	1	rear rays spaced apart
	109	body form lateral view	2	high dorsum, flatter venter
54				
	4	rostral fusion	0	separate bone or bones (no fusion)
	5	rostral numbers	2	single median
	43	maxilla posteroventral process	0	absent
	54	dentition type	1	coronoid-palatal
	79	clavicle length	2	absent
	85	suspensorium	1	limited methyostyly
	99	predorsal ridge scales	0	absent
53				
	1	snout shape	1	sharp bump
	15	narial notches	1	anterior narial notch only
	22	supraorbital canal	2	through/under frontals, supraorbitals lack canal
	36	posterodorsal lo shape	1	T-shaped
	52	marginal tooth orientation	3	pleurodont
	57	preopercular canal dorsally	3	ends blindly in squamosal
	66	anteopercular thickness	1	same as adjacent bones
	69	subopercular height	2	> opercular
	72	first branchiostegal height	1	twice the height of BR2
	89	second dorsal/anal fin rays	3	anterior rays immobile/unjointed
	93	second dorsal fin base	2	guard scales
	94	pectoral fin base	0	endoskeletal axis, unibasal
	105	scale type	3	cycloid
	109	body form lateral view	1	ovoid
	110	highest/lowest points of body profile	3	ridge scale/dorsal fin scales
52				
	16	nasal posterior contact	0	frontal
	25	otic canal bones	2	dermopterotic only (1 bone)
	42	maxilla posterior plate	0	not differentiated from anterior part
	56	dorsal preopercular/squamosal shape	3	tall, narrow
	62	dermohyal	0	absent
51				
	34	posteroventral lo is	2	third
	35	posterodorsal lo is	1	fourth
	36	posterodorsal lo shape	0	narrow rectangular
	38	suborbital fit	2	loose, gaps
	47	posterior maxillary proportions	0	< 0.3

Node	Character		State	
	79	clavicle length	2	absent
	84	parasphenoid	1	length of braincase
	89	second dorsal/anal fin rays	2	all rays spaced apart
	104	caudal fin rays	1	webbed
50 Cladistia				
	11	antorbital presence	0	absent as distinct bone
	12	antorbital shape	0	absent as distinct bone
	14	nasals	0	numerous, serial
	42	maxilla posterior plate	5	absent
	54	dentition type	0	marginal
	81	postspiraculars	1	several, unsutured
	99	predorsal ridge scales	3	complete to occiput
49				
	1	snout shape	0	blunt rounded
	17	supraorbitals	2	single bone
	19	frontals	2	2 pairs
	20	parietal/frontal ratio	0	subequal
	22	supraorbital canal	2	through/under frontals, supraorbitals lack canal
	24	lateral otic margin	2	diverges from midline posteriad
	26	otic-preopercular canal contact	1	present
	30	supraoccipital	2	on skull roof
	37	suborbital bone numbers	2	more than 1 row
	51	mandibular coronoid process	0	absent
	55	preopercular numbers	0	2 subequal
	69	subopercular height	4	subopercular absent
	70	opercular/subopercular anterior margin	4	subopercular absent
	93	second dorsal fin base	1	scaled lobe
48 Holostei				
	3	premaxillary condition	3	sutured to frontals (nasal process)
	44	maxilla mobility	1	free from cheek
	57	preopercular canal dorsally	2	to posterior otic region
	73	branchiostegals below mandible	0	9-12
	82	presupracleithrum	1	absent
	85	suspensorium	2	extensive methyostyly
47				
	25	otic canal bones	1	dermosphenotic and dermopterotic
	37	suborbital numbers	0	none
	38	suborbital fit	0	absent
	39	suborbital thickness	0	absent
	49	supramaxilla	1	present
	105	scale type	1	with pore system
46 Platysomiformes				
	1	snout shape	5	beak
	12	antorbital shape	5	elongate extreme
	45	marginal teeth in upper jaw midline	1	absent
	52	marginal tooth orientation	4	absent
	109	body form, lateral view	4	angulated
45				
	41	maxilla posterior end	1	orbital
	47	posterior maxillary proportions	4	absent
	54	dentition type	2	phyllodont
	72	first branchiostegal height	3	absent
	99	predorsal ridge scales	3	complete to occiput
	110	highest/lowest points of body profile	1	ridge scutes
44				
	24	lateral otic margin	2	diverges from midline posteriad
	42	maxilla posterior plate	3	high triangle
	69	subopercular height	2	> opercular
43				
	37	suborbital numbers	0	none
	38	suborbital fit	0	absent
	39	suborbital thickness	0	absent
42				
	8	ethmoid commissure	2	absent

Node	Character		State	
	16	nasal posterior contact	2	posterodorsal infraorbital
	32	extrascapulars, principle row	4	canal bones only
	96	pelvic fin	2	reduced or absent
	99	predorsal ridge scales	3	complete to occiput
41				
	4	rostral fusion	1	fused to postrostral
	54	dentition type	2	phyllodont
40				
	52	marginal tooth orientation	0	vertical
	53	marginal tooth extent	2	restricted to front
	60	preopercular angle	0	preoperculum absent
	106	scale row inversion	0	progressive
	110	highest/lowest points of body profile	1	ridge scutes

APPENDIX 4

List of taxa included in the phylogenetic analysis.

Name	Source
Holoptychius	Jarvik 1948
Hadronector	Lund & Lund 1985
Allenypterus	Lund & Lund 1985
Cheirolepis trailli	Pearson 1982
Paratarrasius	Lund & Melton 1982
Tarrasius	Taverne 1996
Howqualepis	Long 1988
Mansfieldiscus	Long 1988
Kalops monophrys	Poplin & Lund 2002
Kalops diophrys	Poplin & Lund 2002
Palaeoniscum	Aldinger 1937
E. serratus	Moy-Thomas & Dyne 1938
Wendyichthys	Lund & Poplin 1997
Cyranorhis	Lund & Poplin 1997
Moythomasia	Gardiner 1984
Beagiascus pulcherrimus n. gen., n. sp.	Mickle *et al.* 2009
Roslerichthys	Hamel 2005
Lineagruan judithi n. gen., n. sp.	Mickle *et al.* 2009
L. snowyi n. gen., n. sp.	Mickle *et al.* 2009
Pteronisculus	Nielsen 1942
Canobius	Moy-Thomas & Dyne 1938

Name	Source
Aesopichthys	Poplin & Lund 2000
Proceramala	Poplin & Lund 2000
Roundtail	Lund & Grogan pers. comm.
Spike	Lund. & Grogan pers. comm.
Lepidotes	Woodward 1895; Moy-Thomas & Miles 1971; Tintori 1996
Amia	Grande & Bemis 1998
Calamopleurus	Grande & Bemis 1998
Polypterus	Allis 1922; Pehrson 1947, 1958
Guildayichthys	Lund 2000
Discoserra	Lund 2000
Platysomus gibbosus	Agassiz 1835; Campbell & Phuoc 1983
Platysomus schultzei	Zidek 1992
BGLP	Lund pers. comm.
Amphicentrum	Dyne 1939
Cheirodopsis	Moy-Thomas & Dyne 1938
Platysomus superbus	Moy-Thomas & Dyne 1938
Platysomus striatus	Agassiz 1835; Traquair 1879
Paramesolepis	Moy-Thomas & Dyne 1938

APPENDIX 5

Data matrix. Abbreviations: ***B. pulch.***, *Beagiascus pulcherrimus*; ***C.***, *Cheirolepis*; ***E.***, *Elonichthys*; ***L.***, *Lineagruan*; ***P.***, *Platysomus*.

	0	1	2	3	4	5	6	7	8	9	10	11	12	13	14	15	16	17	18	19	20	21	22	23	24	25	26	27	28	29	30	31	32	33	34	35	36	37	38	39	40	41	42	43	44	45	46	47	48	49	50
Hypothetical Ancestor	0	0	0	0	0	0	0	0	0	0	0	0	0	0	0	0	0	0	0	0	0	0	0	0	0	0	0	0	0	0	0	0	0	0	0	0	0	0	0	0	0	0	0	0	0	0	0	0	0	0	0
Holoptychius	1	0	0	0	0	2	0	0	0	0	0	0	0	0	0	0	0	1	0	0	2	0	2	0	2	1	0	3	0	0	0	0	4	0	0	0	0	0	0	0	0	0	0	0	0	0	0	0	0	0	1
Hadronector	1	0	2	0	0	0	0	0	0	0	0	0	0	0	0	0	0	1	0	0	0	2	0	2	2	1	0	0	0	0	0	0	3	0	1	5	0	0	0	0	0	3	5	0	0	1	3	4	3	0	0
Allenypterus	1	0	2	0	0	0	0	0	0	0	0	0	0	0	0	0	0	0	0	0	0	2	1	2	2	0	0	0	0	0	0	0	0	0	1	5	0	0	0	0	0	3	5	0	0	1	3	4	3	0	0
Roundtail	1	0	0	1	0	2	?	0	0	1	1	1	4	1	2	1	2	3	1	1	1	2	2	0	1	1	0	1	1	1	0	0	0	0	0	0	1	1	1	1	1	0	2	0	0	0	0	3	2	0	1
Spike	1	0	?	?	?	2	?	0	0	1	1	1	4	1	2	1	1	3	1	1	1	2	2	0	1	1	0	0	1	1	0	0	0	0	0	0	1	1	1	1	1	0	2	0	0	0	0	3	2	0	1
C. tralli	0	0	0	0	0	1	0	0	?	1	?	0	0	0	0	2	0	1	0	1	0	0	2	0	0	1	0	0	1	1	0	0	1	0	0	0	1	0	0	0	0	0	1	1	0	0	0	1	0	0	1
Paratarrasius	0	0	0	0	0	2	0	0	0	1	1	1	1	1	1	2	0	3	0	2	1	2	2	2	0	2	0	0	1	1	1	0	1	1	0	0	1	4	1	1	2	0	1	0	0	0	2	1	0	0	1
Tarrasius	1	0	0	0	0	2	0	0	0	1	1	1	1	1	1	?	0	1	0	2	0	2	2	1	0	1	0	0	1	1	0	0	1	0	0	0	2	0	0	0	0	0	2	2	0	0	0	3	0	0	1
Palaeoniscus	0	0	?	0	0	?	0	0	0	2	1	1	1	1	2	1	0	1	1	1	1	2	2	0	0	1	0	0	1	1	0	0	2	0	0	2	0	1	1	1	2	0	1	2	0	?	0	1	0	0	1
E. serratus	0	0	?	?	?	?	0	0	?	1	1	1	1	1	2	1	0	1	1	1	1	2	2	0	0	1	0	1	1	1	0	0	1	0	2	1	2	1	1	1	2	0	1	2	0	?	0	1	0	0	1
Pteronisculus	1	0	0	0	4	4	0	0	1	2	1	1	1	1	2	2	2	3	1	1	1	2	3	0	1	1	0	0	1	1	0	1	2	0	0	1	2	1	1	1	2	0	1	2	0	0	0	1	0	0	1
Moythomasia	1	0	0	?	?	?	0	0	0	?	2	?	?	?	?	2	2	2	3	1	1	0	1	3	0	0	1	0	0	1	1	0	0	2	0	0	0	1	1	1	1	1	0	1	1	0	0	0	1	0	0	1
Howqualepis	0	0	5	4	3	2	2	0	0	1	?	0	0	0	2	2	0	3	1	1	1	1	3	0	?	1	0	0	1	1	0	0	1	0	0	0	1	0	0	0	0	0	1	2	0	0	0	0	0	0	1
Mansfieldiscus	0	0	0	0	0	2	0	0	0	1	1	1	1	1	1	2	0	3	1	1	1	2	3	0	?	1	0	0	1	1	0	0	0	0	0	0	1	1	2	1	?	0	1	2	0	0	0	1	0	0	1
Wendyichthys	0	3	5	4	1	4	1	2	0	2	1	1	2	1	2	1	2	3	1	1	1	2	3	1	1	2	1	0	1	1	0	1	2	0	0	0	1	1	2	2	2	0	1	2	0	1	2	1	0	0	1
Cyranorhis	0	1	5	4	1	4	1	1	0	2	1	1	1	1	2	2	2	3	1	1	1	2	3	0	1	1	?	0	1	1	0	1	2	0	0	0	1	1	1	1	2	0	1	2	0	1	0	1	0	0	1
L. judithi n. gen., n. sp.	0	0	0	0	1	4	0	0	0	2	1	1	2	1	2	2	0	3	1	1	1	2	3	0	0	1	?	0	?	?	0	1	1	2	0	0	1	1	1	1	1	2	0	2	2	0	0	0	0	0	0	1
L. snowyi n. gen., n. sp.	0	0	0	0	1	4	0	0	0	2	1	1	2	1	2	2	0	3	1	1	1	2	3	0	?	1	?	1	?	?	0	?	1	2	0	0	1	1	1	1	1	2	0	1	2	0	0	0	0	0	0	1
B. pulch. n. gen., n. sp.	0	0	1	0	1	4	2	0	0	2	1	1	2	1	2	2	2	3	1	1	1	2	3	0	1	1	1	1	?	?	0	1	1	2	0	0	1	1	1	1	2	0	1	2	0	0	0	0	0	0	1
Roslerichthys	0	0	0	0	?	?	0	0	?	?	?	?	?	?	1	?	?	?	2	1	1	1	?	3	0	1	1	?	0	?	?	0	?	?	?	0	?	?	1	?	?	1	0	1	2	0	0	0	0	0	0	1
Aesopichthys	0	3	3	1	1	4	1	1	0	2	1	1	3	1	2	0	2	3	1	1	1	2	3	0	0	1	?	1	1	1	0	0	0	0	1	0	1	1	1	2	2	1	0	2	2	0	1	2	3	0	0	1
Proceramala	1	0	1	?	?	4	?	?	?	?	?	?	?	1	1	2	2	3	1	1	1	2	3	0	0	1	0	0	1	1	0	?	1	0	0	4	2	2	1	1	1	0	2	2	0	?	0	3	0	0	1
Kalops monophrys	0	0	0	0	0	2	0	0	0	2	1	1	1	1	2	2	0	1	1	1	1	1	2	0	0	1	0	0	1	1	0	1	0	0	0	2	0	1	1	1	2	0	1	2	0	0	0	1	0	0	1
Kalops diophrys	0	0	0	0	0	2	0	0	0	2	1	1	1	1	2	2	0	0	1	1	1	2	2	0	0	1	0	0	1	1	0	1	0	2	0	3	0	2	1	1	2	0	1	2	0	0	0	1	0	0	1
Guildayichthys	1	5	0	1	0	2	0	0	0	?	4	?	0	0	0	0	2	0	2	1	2	0	2	2	0	2	2	1	0	1	1	2	2	0	0	2	3	0	2	2	1	3	1	5	0	0	0	0	0	0	1
Discoserra	1	5	0	1	0	2	0	0	1	3	?	0	0	0	0	2	0	2	1	2	0	2	2	0	2	2	1	0	1	1	2	1	3	0	3	4	0	2	2	1	3	2	5	0	0	0	0	0	0	0	1
Polypterus	1	0	0	2	0	2	0	0	0	4	0	0	0	?	0	0	0	3	1	1	1	2	3	0	0	3	0	2	1	1	0	0	2	0	1	1	0	1	2	1	0	3	5	2	2	0	3	4	3	0	1
Canobius	1	0	0	0	1	4	0	0	0	2	1	1	1	1	2	1	2	3	1	1	1	2	3	0	1	2	?	1	1	1	0	0	1	0	0	0	2	1	1	1	1	0	2	2	0	0	0	2	0	0	1
Amphicentrum	1	5	5	4	0	2	0	0	2	1	1	1	5	2	2	2	2	3	1	1	0	2	3	0	3	2	0	1	1	1	0	0	4	0	0	0	2	0	0	0	0	0	3	0	0	1	0	3	?	0	1
Cheirodopsis	1	5	5	4	4	4	0	0	2	2	2	?	0	5	2	2	1	2	3	1	1	2	3	0	1	2	0	1	1	1	0	0	4	0	2	1	2	0	0	0	0	0	3	0	0	1	0	3	?	0	1
P. superbus	1	5	5	4	1	4	0	0	0	2	1	1	5	2	2	2	0	3	1	1	1	2	3	0	2	2	1	1	1	1	0	0	2	0	0	0	2	0	0	0	0	1	3	0	0	1	0	3	3	0	1
BGLP	1	5	?	1	0	2	0	0	0	2	1	1	5	2	2	1	0	3	1	1	1	2	3	0	2	2	?	1	1	1	0	?	?	?	0	?	2	1	1	1	1	0	3	0	0	1	0	3	3	0	1
P. gibbosus	1	5	5	4	0	2	0	0	2	2	1	1	5	2	2	2	0	3	1	1	1	2	3	0	0	2	0	1	1	1	0	0	2	0	0	3	0	1	1	1	3	1	0	1	0	1	0	4	3	0	1
P. schultzei	1	5	0	0	4	4	0	0	0	?	2	?	1	5	2	2	2	0	3	1	1	1	2	3	0	0	2	0	1	1	1	0	?	?	3	0	0	2	?	1	1	3	1	0	0	0	1	0	4	3	0	1
P. striatus	1	5	5	4	1	2	0	0	0	2	1	1	5	2	2	2	0	3	1	1	1	2	3	0	2	2	1	1	1	1	0	1	2	0	0	0	2	0	0	0	0	0	2	0	0	0	0	0	3	2	0	1
Paramesolepis	0	3	5	4	1	4	0	0	0	2	1	1	3	2	2	2	0	3	1	1	1	2	3	0	0	1	0	0	1	1	0	0	1	0	0	0	2	0	0	0	0	0	0	0	0	1	0	4	0	0	1
Amia	1	0	0	3	0	2	0	0	0	4	1	1	4	1	2	0	0	3	1	1	1	2	3	0	0	1	0	0	1	1	0	0	1	0	2	1	3	0	0	0	3	0	0	0	0	1	0	2	0	0	1
Calamopleurus	1	0	0	3	0	2	0	0	0	5	1	1	4	1	2	0	0	0	1	1	1	2	3	0	0	1	0	0	1	1	0	0	1	0	2	1	0	0	0	0	3	0	0	0	0	1	0	0	0	1	1
Lepidotes	1	0	0	3	0	2	0	0	0	5	1	1	4	2	2	0	0	1	1	1	1	2	3	0	0	2	0	1	1	1	0	1	1	0	3	4	0	1	2	1	1	2	0	0	1	1	0	0	3	0	1

Appendix 5 (continuation).

	51	52	53	54	55	56	57	58	59	60	61	62	63	64	65	66	67	68	69	70	71	72	73	74	75	76	77	78	79	80	81	82	83	84	85	86	87	88	89	90	91	92	93	94	95	96	97	98	99	100
Hypothetical Ancestor	0	0	0	0	0	0	0	0	0	0	0	0	0	0	0	0	0	0	0	0	0	0	0	0	0	0	0	0	0	0	0	0	0	0	0	0	0	0	0	0	0	0	0	0	0	0	0	0	0	0
Holoptychius	0	0	0	1	0	0	1	0	0	0	0	0	0	0	0	0	0	1	2	0	0	0	3	0	0	2	0	0	0	0	0	0	?	0	0	0	1	2	0	0	0	0	3	0	0	0	0	1	0	0
Hadronector	1	0	0	0	0	0	3	0	0	0	0	0	0	0	0	0	1	1	0	0	0	3	3	1	0	1	3	1	0	0	0	0	0	0	0	0	0	0	2	0	0	0	3	0	0	0	2	2	0	0
Allenypterus	1	0	0	0	0	0	3	0	0	0	0	0	0	0	0	0	1	1	0	0	0	3	3	1	0	1	3	1	0	0	0	0	0	0	0	0	0	0	2	0	0	0	3	0	0	0	2	3	0	0
Roundtail	1	3	2	1	1	2	3	0	2	1	2	1	0	0	0	1	0	1	2	0	0	1	3	2	0	1	0	1	?	0	0	?	1	0	1	1	2	0	3	1	2	4	2	0	0	0	1	2	1	2
Spike	1	3	1	1	1	2	3	0	2	1	2	1	0	0	0	1	0	1	2	0	0	1	3	3	0	1	0	1	0	0	0	?	1	0	1	1	2	0	3	1	2	4	2	0	0	0	1	2	0	1
C. tralli	0	0	0	0	2	1	0	0	2	4	3	1	0	0	0	0	0	1	0	3	0	0	0	0	0	0	0	1	?	0	0	0	1	?	?	1	2	2	0	0	0	0	0	1	1	0	0	0	0	?
Paratarrasius	0	0	0	0	1	1	0	0	1	2	2	3	0	0	0	0	1	1	0	0	0	0	3	0	0	0	0	1	?	0	0	0	0	0	2	1	2	0	2	2	2	2	0	1	0	2	2	3	0	0
Tarrasius	?	0	0	0	1	1	0	0	1	1	2	1	0	0	0	0	0	0	0	0	0	0	2	0	0	?	?	1	?	0	0	0	?	0	?	1	2	0	2	2	2	1	0	1	0	2	2	3	0	0
Palaeoniscum	0	0	0	0	1	1	0	0	1	3	?	0	0	0	0	0	0	1	1	1	0	0	1	0	0	0	0	1	?	0	0	1	?	0	?	1	2	2	0	0	0	0	0	1	1	0	0	1	1	?
E. serratus	0	0	0	0	1	1	0	0	1	3	?	0	0	0	0	0	2	0	0	1	0	0	2	0	0	?	?	1	?	0	0	?	?	?	?	1	2	?	?	0	0	0	0	1	1	0	0	1	1	?
Pteronisculus	0	0	0	0	1	1	0	0	1	3	?	1	0	0	0	0	1	0	0	1	0	0	0	0	0	0	0	1	1	0	0	0	1	0	2	1	2	0	0	0	0	0	0	1	1	0	0	0	1	?
Moythomasia	0	0	0	0	1	1	0	0	1	4	?	1	2	2	2	1	2	0	0	1	0	0	0	0	0	0	0	1	1	0	0	0	1	0	?	1	2	0	0	0	0	0	2	1	1	0	0	1	3	?
Howqualepis	0	0	0	0	2	1	0	0	1	4	1	1	0	0	0	0	0	0	0	0	0	1	0	0	0	0	0	1	1	0	0	0	1	0	2	1	2	0	0	0	0	0	0	1	1	1	0	0	1	1
Mansfieldiscus	0	0	0	0	1	1	1	0	1	?	?	2	0	0	0	0	?	?	?	?	0	0	0	0	0	0	0	1	?	?	0	0	1	?	?	1	2	0	0	0	0	0	0	1	1	0	0	0	1	?
Wendyichthys	0	1	0	0	1	1	0	0	1	3	2	1	0	0	0	0	3	4	0	0	0	1	0	0	1	1	0	1	1	0	0	0	1	0	2	1	2	0	0	0	0	0	2	1	1	0	0	0	1	1
Cyranorhis	0	1	0	0	1	1	0	0	1	3	2	1	0	0	0	0	0	0	0	1	0	0	0	0	1	1	0	1	1	0	0	0	1	0	2	1	2	0	0	0	0	0	2	1	1	0	0	0	1	1
L. judithi n. gen., n. sp.	0	0	0	0	1	1	0	0	1	2	2	1	2	2	1	2	3	4	0	1	0	0	2	1	1	0	0	1	1	0	3	0	1	0	2	1	2	0	0	0	0	0	2	1	1	0	0	0	1	1
L. snowyi n. gen., n. sp.	0	1	0	0	1	1	0	0	1	2	2	1	2	3	1	2	3	4	0	1	0	1	0	1	1	0	0	1	1	0	3	0	1	?	2	1	2	0	0	0	0	0	2	1	1	0	0	0	1	1
B. pulch. n. gen., n. sp.	0	2	0	0	1	1	0	0	1	2	2	1	2	2	2	1	4	2	0	1	0	1	0	1	1	0	0	1	1	0	2	0	1	?	2	1	2	1	0	0	0	0	0	1	1	0	0	0	1	2
Roslerichthys	0	?	0	0	1	?	?	0	1	?	?	1	2	1	3	1	1	4	0	0	0	0	?	?	?	?	?	1	?	?	?	0	1	?	2	1	2	0	0	0	0	0	0	1	1	?	0	?	?	1
Aesopichthys	1	0	0	0	1	2	0	0	1	1	2	1	0	0	0	0	1	2	0	0	0	2	3	0	?	?	?	1	1	0	0	0	1	?	2	1	2	0	1	1	1	0	1	1	0	0	0	0	2	1
Proceramala	1	0	0	0	1	1	0	0	1	1	1	1	0	0	0	0	0	1	0	0	0	0	3	0	?	?	?	1	?	0	0	0	1	?	2	1	2	0	1	1	1	0	0	1	0	0	0	0	3	1
Kalops monophrys	0	0	0	0	1	1	0	0	1	3	1	1	0	0	0	0	0	2	0	1	0	1	0	0	0	1	0	1	0	0	0	0	1	?	2	1	2	0	1	0	1	0	0	1	0	0	0	0	3	2
Kalops diophrys	0	0	0	0	1	1	0	0	1	3	1	1	0	0	0	0	0	1	0	1	0	0	0	0	0	1	0	1	0	0	0	0	1	?	2	1	2	0	1	0	1	0	0	1	0	0	0	0	1	2
Guildayichthys	0	0	1	0	0	3	0	0	1	0	3	0	0	0	0	0	5	5	4	4	1	0	3	2	0	0	0	1	?	0	1	0	0	1	1	1	2	0	3	1	2	1	1	1	0	0	0	2	3	2
Discoserra	0	0	2	0	0	3	0	0	1	0	3	0	0	0	0	0	5	5	4	4	1	0	3	2	0	0	0	1	?	0	1	0	0	1	1	1	2	0	2	1	2	1	1	1	0	2	0	2	3	2
Polypterus	1	4	3	0	1	0	0	0	4	0	?	1	0	0	0	0	4	0	0	0	0	3	3	3	0	2	3	1	2	0	1	?	?	1	1	1	2	0	2	1	2	4	0	1	0	0	1	2	3	?
Canobius	0	0	0	0	1	2	0	0	1	1	1	1	0	0	0	0	1	1	2	0	0	0	2	0	0	1	1	1	?	0	0	?	3	?	?	1	2	1	0	0	0	0	0	1	1	0	0	1	2	2
Amphicentrum	?	4	3	1	1	3	0	0	2	1	3	0	0	0	0	0	0	0	2	0	0	0	3	0	0	?	?	1	0	0	0	?	?	0	1	1	2	2	0	1	1	2	0	0	3	?	0	0	0	3	?
Cheirodopsis	?	4	3	1	1	2	0	0	2	1	1	1	0	0	0	0	0	0	2	0	0	0	3	0	0	?	?	1	0	0	0	1	?	?	?	1	2	0	0	1	0	0	0	0	1	1	2	0	1	3	0
P. superbus	0	4	3	2	1	3	0	0	2	1	3	0	0	0	0	0	0	1	2	0	0	0	2	0	0	0	1	1	0	0	0	1	?	0	?	1	2	0	0	1	2	3	0	1	1	0	0	0	0	2
BGLP	1	4	3	1	1	3	0	0	2	1	1	0	0	0	0	0	0	1	2	0	0	0	?	0	0	?	?	1	0	0	0	?	1	0	1	1	2	0	0	1	2	3	0	1	1	0	0	0	0	2
P. gibbosus	1	4	3	2	2	3	2	2	1	1	3	0	0	0	0	0	5	5	4	4	0	3	3	3	0	?	?	1	0	0	0	0	?	?	?	1	2	0	0	1	2	2	0	1	1	0	0	0	3	?
P. schultzei	?	4	3	2	?	3	0	?	2	0	?	0	0	0	0	0	2	4	0	0	0	3	3	3	0	?	?	1	0	0	0	0	1	?	?	1	2	1	1	1	2	2	0	1	1	1	2	0	0	3	?
P. striatus	?	0	2	2	1	3	0	0	2	0	3	0	0	0	0	0	0	0	1	0	0	0	3	0	0	?	?	1	0	0	0	1	?	?	?	1	2	?	?	1	2	2	0	1	1	2	0	0	0	?
Paramesolepis	0	0	2	0	1	3	0	0	2	0	3	1	0	0	0	0	2	0	2	0	0	0	3	0	0	?	?	1	?	0	0	?	3	?	?	1	2	0	0	1	1	0	0	1	1	0	0	1	3	2
Amia	1	0	0	1	1	3	2	0	3	0	3	0	0	0	0	0	1	0	0	0	1	0	0	0	0	1	3	1	2	0	0	1	3	1	2	1	2	0	2	1	2	1	0	1	1	0	1	2	0	0
Calamopleurus	1	0	0	1	1	3	2	0	3	0	3	0	0	0	0	0	0	4	0	0	1	1	0	0	0	1	3	1	2	0	0	1	2	1	2	1	2	0	2	0	0	0	0	1	1	0	1	2	0	0
Lepidotes	1	0	?	1	1	3	2	0	3	1	3	0	0	0	0	0	0	1	0	0	1	1	0	0	0	1	3	1	2	0	0	1	?	?	2	1	2	0	2	0	0	0	0	1	1	0	1	0	0	?

Appendix 5 (continuation).

	101	102	103	104	105	106	107	108	109	110
Hypothetical Ancestor	0	0	0	0	0	0	0	0	0	0
Holoptychius	0	0	0	0	1	2	0	0	1	0
Hadronector	0	0	0	1	1	2	0	0	1	0
Allenypterus	0	0	0	1	1	2	0	0	2	0
Roundtail	0	1	1	0	3	1	0	0	1	3
Spike	1	1	1	0	3	1	0	0	1	3
C. tralli	?	1	0	0	0	0	3	2	0	0
Paratarrasius	0	1	2	0	0	1	3	2	0	0
Tarrasius	0	1	2	1	0	2	3	2	0	0
Palaeoniscum	?	1	0	0	0	1	0	0	0	0
E. serratus	?	1	1	0	0	0	?	?	0	?
Pteronisculus	?	1	0	0	0	1	?	?	0	0
Moythomasia	?	1	0	0	0	1	?	?	0	0
Howqualepis	1	1	0	0	0	0	0	0	0	0
Mansfieldiscus	?	1	0	0	0	0	?	?	0	0
Wendyichthys	1	1	0	0	0	1	0	1	0	0
Cyranorhis	1	1	0	0	0	0	0	1	0	0
L. judithi n. gen., n. sp.	1	1	0	0	0	1	0	1	0	0
L. snowyi n. gen., n. sp.	1	1	0	0	0	1	0	1	0	0
B. pulch. n. gen., n. sp.	2	1	0	0	0	1	0	1	0	0
Roslerichthys	0	1	0	0	0	1	0	1	0	0
Aesopichthys	2	1	0	1	0	1	0	0	2	0
Proceramala	1	1	1	0	0	1	0	0	2	0
Kalops monophrys	1	1	0	0	0	1	0	0	0	0
Kalops diophrys	1	1	0	0	0	1	0	1	0	0
Guildayichthys	2	1	1	1	0	1	0	0	3	3
Discoserra	2	1	1	1	0	1	1	0	3	1
Polypterus	?	1	0	1	0	2	0	0	0	0
Canobius	1	1	1	0	0	0	0	0	0	1
Amphicentrum	?	1	1	0	0	1	0	0	4	2
Cheirodopsis	0	1	1	0	0	1	0	0	3	0
P. superbus	0	1	1	0	0	1	0	0	4	0
BGLP	0	1	1	0	0	1	0	0	4	0
P. gibbosus	?	1	1	0	0	?	0	0	4	1
P. schultzei	?	1	1	0	0	0	0	0	3	1
P. striatus	?	1	1	0	0	0	0	0	4	1
Paramesolepis	2	1	0	0	0	0	0	0	2	1
Amia	0	1	0	1	1	2	0	0	0	0
Calamopleurus	0	1	0	1	1	2	0	0	0	0
Lepidotes	?	0	0	1	0	2	0	0	2	0